18. Travis WD, Elisabeth B, Muller-Hermelink HK, Harris CC: *Pathology and Geneticsof Tumours of the Lung, Pleural, Thymus and Heart.* Lyon: IARC press; 2004.
19. AJCC: *Cancer Staging Manual.* 6th edition; 2002:167–177. Chapter 19; Lung - original pages.
20. Ishikawa Y, Furuta R, Miyoshi T, Satoh Y, Okumura S, Nakagawa K, Tsuchiya E: **Loss of heterozygosity and the smoking index increase with decrease in differentiation of lung adenocarcinomas: etiologic implications.** *Cancer Lett* 2002, **187**:47–51.
21. Nannya Y, Sanada M, Nakazaki K, Hosoya N, Wang L, Hangaishi A, Kurokawa M, Chiba S, Bailey DK, Kennedy GC, Ogawa S: **A robust algorithm for copy number detection using high-density oligonucleotide single nucleotide polymorphism genotyping arrays.** *Cancer Res* 2005, **65**:6071–6079.
22. Ogawa S, Nanya Y, Yamamoto G: **Genome-wide copy number analysis on GeneChip platform using copy number analyzer for affymetrix GeneChip 2.0 software.** *Meth Mol Biol* 2007, **396**:185–206.
23. Yamamoto G, Nannya Y, Kato M, Sanada M, Levine RL, Kawamata N, Hangaishi A, Kurokawa M, Chiba S, Gilliland DG, Koeffler HP, Ogawa S: **Highly sensitive method for genomewide detection of allelic composition in nonpaired, primary tumor specimens by use of affymetrix single-nucleotide-polymorphism genotyping microarrays.** *Am J Hum Genet* 2007, **81**:114–126.
24. Danner BC, Gerdes JS, Jung K, Sander B, Enders C, Liersch T, Seipelt R, Gutenberg A, Gunawan B, Schöndube FA, Füzesi L: **Comparison of chromosomal aberrations in primary colorectal carcinomas to their pulmonary metastases.** *Canc Genet* 2011, **204**:122–128.
25. Weir BA, Woo MS, Getz G, Perner S, Ding L, Beroukhim R, Lin WM, Province MA, Kraja A, Johnson LA, Shah K, Sato M, Thomas RK, Barletta JA, Borecki IB, Broderick S, Chang AC, Chiang DY, Chirieac LR, Cho J, Fujii Y, Gazdar AF, Giordano T, Greulich H, Hanna M, Johnson BE, Kris MG, Lash A, Lin L, Lindeman N, *et al*: **Characterizing the cancer genome in lung adenocarcinoma.** *Nature* 2007, **450**:893–898.
26. Kwei KA, Kim YH, Girard L, Kao J, Pacyna-Gengelbach M, Salari K, Lee J, Choi YL, Sato M, Wang P, Hernandez-Boussard T, Gazdar AF, Petersen I, Minna JD, Pollack JR: **Genomic profiling identifies TITF1 as a lineage-specific oncogene amplified in lung cancer.** *Oncogene* 2008, **27**:3635–3640.
27. Sasaki H, Hikosaka Y, Kawano O, Moriyama S, Yano M, Fujii Y: **Evaluation of Kras gene mutation and copy number gain in non-small cell lung cancer.** *J Thorac Oncol* 2011, **6**:15–20.
28. Reinersman JM, Johnson ML, Riely GJ, Chitale DA, Nicastri AD, Soff GA, Schwartz AG, Sima CS, Ayalew G, Lau C, Zakowski MF, Rusch VW, Ladanyi M, Kris MG: **Frequency of EGFR and KRAS mutations in lung adenocarcinomas in African Americans.** *J Thorac Oncol* 2011, **6**:28–31.
29. Kosaka T, Yatabe Y, Onozato R, Kuwano H, Mitsudomi T: **Prognostic implication of EGFR, KRAS, and TP53 gene mutations in a large cohort of Japanese patients with surgically treated lung adenocarcinoma.** *J Thorac Oncol* 2009, **4**:22–29.
30. Kohno T, Otsuka A, Girard L, Sato M, Iwakawa R, Ogiwara H, Sanchez-Cespedes M, Minna JD, Yokota J: **A catalog of genes homozygously deleted in human lung cancer and the candidacy of PTPRD as a tumor suppressor gene.** *Gene Chromosome Canc* 2010, **49**:342–352.
31. Veeriah S, Brennan C, Meng S, Singh B, Fagin JA, Solit DB, Paty PB P, Rohle D, Vivanco I, Chmielecki J, Pao W, Ladanyi M, Gerald WL, Liau L, Cloughesy TC, Mischel PS, Sander C, Taylor B, Schultz N, Major J, Heguy A, Fang F, Mellinghoff IK, Chan TA: **The tyrosine phosphatase PTPRD is a tumor suppressor that is frequently inactivated and mutated in glioblastoma and other human cancers.** *Proc Natl Acad Sci USA* 2009, **106**:9435–9440.
32. Tomlins SA, Laxman B, Dhanasekaran SM, Helgeson BE, Cao X, Morris DS, Menon A, Jing X, Cao Q, Han B, Yu J, Wang L, Montie JE, Rubin MA, Pienta KJ, Roulston D, Shah RB, Varambally S, Mehra R, Chinnaiyan AM: **Distinct classes of chromosomal rearrangements create oncogenic ETS gene fusions in prostate cancer.** *Nature* 2007, **448**:595–599.
33. Kato M, Sanada M, Kato I, Sato Y, Takita J, Takeuchi K, Niwa A, Chen Y, Nakazaki K, Nomoto J, Asakura Y, Akatsuka M, Hayashi Y, Mori H, Igarashi T, Kurokawa M, Chiba S, Mori S, Ishikawa Y, Okamoto K, Tobinai K, Nakagama H, Nakahata T, Yoshino T, Kobayashi Y, Ogawa S: **Frequent inactivation of A20 in B-cell lymphomas.** *Nature* 2009, **459**:712–716.
34. Sanada M, Suzuki T, Shih LY, Otsu M, Kato M, Yamazaki S, Tamura A, Honda H, Sakata-Yanagimoto M, Kumano K, Oda H, Yamagata T, Takita J, Gotoh N, Nakazaki K, Kawamata N, Onodera M, Nobuyoshi M, Hayashi Y, Harada H, Kurokawa M, Chiba S, Mori H, Ozawa K, Omine M, Hirai H, Nakauchi H, Koeffler HP, Ogawa S: **Gain-of-function of mutated C-CBL tumour suppressor in myeloid neoplasms.** *Nature* 2009, **460**:904–908.
35. Ninomiya H, Nomura K, Satoh Y, Okumura S, Nakagawa K, Fujiwara M, Tsuchiya E, Ishikawa Y: **Genetic instability in lung cancer: concurrent analysis of chromosomal, mini- and microsatellite instability and loss of heterozygosity.** *Br J Cancer* 2006, **94**:1485–1491.
36. Yoshino I, Fukuyama S, Kameyama T, Shikada Y, Oda S, Maehara Y, Sugimachi K: **Detection of loss of heterozygosity by high-resolution fluorescent system in non-small cell lung cancer: association of loss of heterozygosity with smoking and tumor progression.** *Chest* 2003, **123**:545–550.
37. Yohena T, Yoshino I, Takenaka T, Ohba T, Kouso H, Osoegawa A, Hamatake M, Oda S, Kuniyoshi Y, Maehara Y: **Relationship between the loss of heterozygosity and tobacco smoking in pulmonary adenocarcinoma.** *Oncol Res* 2007, **16**:333–339.
38. Le Calvez F, Mukeria A, Hunt JD, Kelm O, Hung RJ, Tanière P, Brennan P, Boffetta P, Zaridze DG, Hainaut P: **TP53 and KRAS mutation load and types in lung cancers in relation to tobacco smoke: distinct patterns in never, former, and current smokers.** *Cancer Res* 2005, **65**:5076–5083.
39. Gazdar AF, Shigematsu H, Herz J, Minna JD: **Mutations and addiction to EGFR: the Achilles 'heal' of lung cancers?** *Trends Mol Med* 2004, **10**:481–486.
40. Woodburn JR: **The epidermal growth factor receptor and its inhibition in cancer therapy.** *Pharmacol Ther* 1999, **82**:241–250.
41. Cappuzzo F, Varella-Garcia M, Shigematsu H, Domenichini I, Bartolini S, Ceresoli GL, Rossi E, Ludovini V, Gregorc V, Toschi L, Franklin WA, Gazdar AF CL, Bunn PA Jr, Hirsch FR: **Increased HER2 gene copy number is associated with response to gefitinib therapy in epidermal growth factor receptor-positive non-small-cell lung cancer patients.** *J Clin Oncol* 2005, **23**:5007–5018.
42. Varella-Garcia M, Mitsudomi T, Yatabe Y: **EGFR and HER2 genomic gain in recurrent non-small cell lung cancer after surgery: impact on outcome to treatment with gefitinib and association with EGFR and KRAS mutations in a Japanese cohort.** *J Thorac Oncol* 2009, **4**:318–325.
43. Pugh TJ, Bebb G, Barclay L, Sutcliffe M, Fee J, Salski C, O'Connor R, Ho C, Murray N, Melosky B, English J, Vielkind J, Horsman D, Laskin JJ, Marra MA: **Correlations of EGFR mutations and increases in EGFR and HER2 copy number to gefitinib response in a retrospective analysis of lung cancer patients.** *BMC Canc* 2007, **7**:128.
44. Blons H, Pallier K, Le Corre D, Danel C, Tremblay-Gravel M, Houdayer C, Fabre-Guillevin E, Riquet M, Dessen P, Laurent-Puig P: **Genome wide SNP comparative analysis between EGFR and KRAS mutated NSCLC and characterization of two models of oncogenic cooperation in non-small cell lung carcinoma.** *BMC Med Genom* 2008, **1**:25.
45. Zhang A, Zheng C, Lindvall C, Hou M, Ekedahl J, Lewensohn R, Yan Z, Yang X, Henriksson M, Blennow E, Nordenskjöld M, Zetterberg A, Björkholm M, Gruber A, Xu D: **Frequent amplification of the telomerase reverse transcriptase gene in human tumors.** *Cancer Res* 2000, **60**:6230–6235.
46. Saretzki G, Petersen S, Petersen I, Kölble K, von Zglinicki T: **hTERT gene dosage correlates with telomerase activity in human lung cancer cell lines.** *Cancer Lett* 2002, **176**:81–91.
47. Kang JU, Koo SH, Kwon KC, Park JW, Kim JM: **Gain at chromosomal region 5p15.33, containing TERT, is the most frequent genetic event in early stages of non-small cell lung cancer.** *Canc Genet Cytogenet* 2008, **182**:1–11.
48. Hsiung CA, Lan Q, Hong YC, Chen CJ, Hosgood HD, Chang IS, Chatterjee N, Brennan P, Wu C, Zheng W, Chang GC, Wu T, Park JY, Hsiao CF, Kim YH, Shen H, Seow A, Yeager M, Tsai YH, Kim YT, Chow WH, Guo H, Wang WC, Sung SW, Hu Z, Chen KY, Kim JH, Chen Y, Huang L, Lee KM, *et al*: **The 5p15.33 locus is associated with risk of lung adenocarcinoma in never-smoking females in Asia.** *PLoS Genet* 2010, **6**:e1001051.
49. McKay JD, Hung RJ, Gaborieau V, Boffetta P, Chabrier A, Byrnes G, Zaridze D, Mukeria A, Szeszenia-Dabrowska N, Lissowska J, Rudnai P, Fabianova E, Mates D, Bencko V, Foretova L, Janout V, McLaughlin J, Shepherd F, Montpetit A, Narod S, Krokan HE, Skorpen F, Elvestad MB, Vatten L, Njølstad

I, Axelsson T, Chen C, Goodman G, Barnett M, Loomis MM, *et al*: **Lung cancer susceptibility locus at 5p15.33.** *Nat Genet* 2008, **40**:1404–1406.

50. Camidge DR, Theodoro M, Maxson DA, Skokan M, O'Brien T, Lu X, Doebele RC, Barón AE, Varella-Garcia M: **Correlations between the percentage of tumor cells showing an anaplastic lymphoma kinase (ALK) gene rearrangement, ALK signal copy number, and response to crizotinib therapy in ALK fluorescence in situ hybridization-positive nonsmall cell lung cancer.** *Cancer* 2012, **118**:4486–4494.

doi:10.1186/1471-2407-13-8
Cite this article as: Ninomiya *et al.*: Allelotypes of lung adenocarcinomas featuring *ALK* fusion demonstrate fewer onco- and suppressor gene changes. *BMC Cancer* 2013 13:8.

Submit your next manuscript to BioMed Central and take full advantage of:

- Convenient online submission
- Thorough peer review
- No space constraints or color figure charges
- Immediate publication on acceptance
- Inclusion in PubMed, CAS, Scopus and Google Scholar
- Research which is freely available for redistribution

Submit your manuscript at
www.biomedcentral.com/submit

BioMed Central

The HSP90 inhibitor 17-N-allylamino-17-demethoxy geldanamycin (17-AAG) synergizes with cisplatin and induces apoptosis in cisplatin-resistant esophageal squamous cell carcinoma cell lines via the Akt/XIAP pathway

TAKASHI UI[1], KAZUE MORISHIMA[1], SHIN SAITO[1], YUJI SAKUMA[2], HIROFUMI FUJII[3], YOSHINORI HOSOYA[1], SHUMPEI ISHIKAWA[4], HIROYUKI ABURATANI[5], MASASHI FUKAYAMA[6], TOSHIRO NIKI[2] and YOSHIKAZU YASUDA[1]

Departments of [1]Surgery, [2]Pathology and [3]Clinical Oncology, Jichi Medical University, Shimotsuke, Tochigi 329-0498; [4]Division of Genomic Pathology, Medical Research Institute, Tokyo Medical and Dental University, Bunkyo-ku, Tokyo 113-8510; [5]Division of Genome Science, Research Center for Advanced Science and Technology, the University of Tokyo, Meguro-ku, Tokyo 153-8904; [6]Department of Pathology, Graduate School of Medicine, the University of Tokyo, Bunkyo-ku, Tokyo 113-0033, Japan

Received October 9, 2013; Accepted November 20, 2013

DOI: 10.3892/or.2013.2899

Abstract. Although cisplatin (CDDP) is a key drug in the treatment of esophageal squamous cell carcinoma (ESCC), acquired chemoresistance remains a major problem. Combination therapy may represent one strategy to overcome this resistance. Heat shock protein 90 (HSP90) is known to be overexpressed in several types of cancer cells, and its inhibition by small molecules, either alone or in combination, has shown promise in the treatment of solid malignancies. In the present study, we evaluated the synergistic effects of combining CDDP with the HSP90 inhibitor 17-N-allylamino-17-demethoxy geldanamycin (17-AAG) on two CDDP-resistant human esophageal squamous cancer cell lines, KYSE30 and KYSE150. The results obtained demonstrated the synergistic inhibitory effects of CDDP and 17-AAG on the growth of KYSE30 and KYSE150 cells. Cell growth and cell number were more effectively reduced by the combined treatment with CDDP and 17-AAG than by the treatment with either CDDP or 17-AAG alone. Western blotting revealed that the combined action of CDDP and 17-AAG cleaved poly (ADP-ribose) polymerase (PARP) and caspase-3, which demonstrated that the reduction in both cell growth and cell number was mediated by apoptosis. Time-course experiments showed that reduction in X-linked inhibitor of apoptosis protein (XIAP) and phosphorylated Akt were concomitant with apoptosis. The results of the present study demonstrate that 17-AAG synergizes with CDDP and induces apoptosis in CDDP-resistant ESCC cell lines, and also that modulation of the Akt/XIAP pathway may underlie this synergistic effect. Combination therapy with CDDP and an HSP90 inhibitor may represent a promising strategy to overcome CDDP resistance in ESCC.

Correspondence to: Professor Toshiro Niki, Department of Pathology, Jichi Medical University, 3311-1 Yakushiji, Shimotsuke, Tochigi, 329-0498, Japan
E-mail: tniki@jichi.ac.jp

Key words: cisplatin, tanespimycin, HSP90 heat shock protein inhibitor, esophageal squamous cell carcinoma

Introduction

Esophageal cancer is one of the most aggressive types of cancer of the gastrointestinal tract. The estimated incidence of esophageal cancer was 3.8% of all cancers and the estimated cancer mortality worldwide was 5.4% in 2008 (1). The incidence of esophageal cancer is particularly high in both males and females in East Asia, with squamous cell carcinoma being the predominant histologic type in this region, accounting for more than 90% of all esophageal cancer cases (1). Multimodality therapy, including surgery, chemotherapy and radiotherapy, is required for the effective management of advanced esophageal cancer. However, the 5-year survival rates of patients treated using surgery, chemotherapy alone, radiotherapy alone and concurrent chemoradiotherapy were reported to be 50.2, 8.6, 15.5 and 26.4%, respectively (2). Therefore, further improvements in outcomes are urgently required (2-5).

Cisplatin (CDDP) is a platinum drug that is widely used to treat esophageal squamous cell carcinoma (ESCC) (6,7). CDDP, either alone or in combination with other agents, has been shown to improve patient outcomes. However, acquired chemoresistance develops during the course of treatment and is often the reason for treatment failure. Therefore, overcoming chemoresistance is essential for improving the outcomes of patients.

Molecular chaperone proteins function to ensure the proper conformation of client proteins when cells experience stress or damage (8). Heat shock protein 90 (HSP90) is a molecular chaperone that participates in stabilizing and activating more than 200 proteins, including serine/threonine kinases (Akt, Raf-1, and Cdk4), and the transcription factors hypoxia-inducible factor 1α (HIF1α) and p53, receptor/non-receptor kinases (HER2, EGFR, and Src family kinases), and steroid hormone receptors (9). Since many of these client proteins have been shown to significantly contribute to tumor growth and survival, abrogating their function with an HSP90 inhibitor is an attractive prospect (10).

In this study, we explored the potential synergistic effect of CDDP and the HSP90 inhibitor, 17-N-allylamino-17-demethoxy geldanamycin (17-AAG), on human ESCC cell lines. We also attempted to identify the molecular mechanism involved in this synergistic effect.

Materials and methods

Cell lines and culture. The TE series (TE1, TE4, TE5, TE6, TE8, TE9, TE10, TE11, TE14 and TE15) and EC-GI-10 were obtained from the Riken BioResource Center (Saitama, Japan). The KYSE series (KYSE30, KYSE70, KYSE140, KYSE150, KYSE170, KYSE180, KYSE220 and KYSE270), TT, and TTn were obtained from the Health Science Foundation (Tokyo, Japan). These cell lines were derived from human esophageal squamous cancer. Cells were cultured in a 5% CO_2 atmosphere at 37°C in RPMI-1640 (R8758; Sigma-Aldrich, St. Louis, MO, USA) complete medium supplemented with 10% fetal bovine serum (FBS), penicillin (100 U/ml), and streptomycin (100 μg/ml).

Chemicals and antibodies. CDDP and 17-AAG were purchased from Sigma-Aldrich. CDDP was dissolved in 0.9% sodium chloride solution and 17-AAG was dissolved in dimethyl sulfoxide (DMSO). All drugs were stored in aliquots at -20°C.

Antibodies to caspase-3 (#9662), PARP (#9542), XIAP (3B6) (#2045), c-IAP1 (#4952), c-IAP2 (58C7) (#3130), livin (D61D1) XP (#5471), survivin (71G4B7) (#2808), phospho-Akt (Ser473) (D9E) (#4060), Akt (#9272), phospho-p44/42 MAPK (Erk1/2) (Thr202/Tyr204) (#9101), and p44/p22 MAPK (Erk1/2) (#9102) were from Cell Signaling Technologies (Beverly, MA, USA). The antibody to β-actin was from Sigma-Aldrich. Antibodies to Bcl-2 (#610391), Bcl-xL (#60982), Bid (#61158), Bad (#610391), Bax (#610982), Beclin (#612112), and BAG-1 (#611868) were from BD Biosciences (San Jose, CA, USA).

Drug sensitivity assay. Cells were suspended in RPMI/10% FBS and seeded at between 2,000 and 4,000 cells/well in quintuplicate in 96-well plates. Cells were treated with varying doses of CDDP and 17-AAG 24 h after plating and were allowed to grow for an additional 72 h. Viable cell density was determined by a water-soluble tetrazolium salt (WST-8, Cell Counting kit-8; Dojindo, Japan) according to the manufacturer's instructions using a microplate absorbance reader (Bio-Rad Laboratories, Hercules, CA, USA) at 450 nm.

Determination of IC_{50} and combination index (CI). IC_{50} was calculated using the CompuSyn software (ComboSyn, Inc., Paramus, NJ, USA). CI values were calculated for 50% toxicity based on the equation below (11):

$$CI = D_1 / Dx_1 + D_2 / Dx_2 + \alpha \times [(D_1 \times D_2) / (Dx_1 \times Dx_2)]$$

where, Dx_1 = Dose of drug 1 to produce 50% cell kill alone; D_1 = Dose of drug 1 to produce 50% cell kill in combination with D_2; Dx_2 = Dose of drug 2 to produce 50% cell kill alone; D_2 = Dose of drug 2 to produce 50% cell kill in combination with D_1; α=0 for mutually exclusive or 1 for mutually non-exclusive modes of drug action.

Time-dependent cell growth assay. Equal numbers of cells were seeded in quintuplicate in 96-well plates and cell growth was measured using WST-8 Cell Counting kit-8 at 0, 24, 48 and 72 h. The results were expressed as percentages relative to the absorbance at 0 h.

Western blot analysis. KYSE30 and KYSE150 cells were seeded on 100 mm plates and were exposed to CDDP with/without 17-AAG after 24 h. Cells were subsequently cultured for 24, 48 and 72 h; adherent and floating cells were then pelleted, washed with cold PBS and lysed in RIPA buffer [150 mM NaCl, 20 mM Tris-HCl (pH 7.5), 50 mM NaF, 20 μM Na_3VO_4 and protease inhibitor]. Lysates were centrifuged at 15,000 rpm at 4°C for 10 min and the protein concentration in each sample was determined by the BCA Protein Assay kit (Takara Bio, Inc., Shiga, Japan). Cell lysates or their fractions containing equal amounts of protein (12 μg) were resolved by the Mini-Protean TGX Precast Gel (Bio-Rad Laboratories) and transferred to nitrocellulose membranes. Membranes were probed with the primary antibody, followed by the secondary antibody conjugated to HRP, developed using western blot detection reagents (Amersham Biosciences, Uppsala, Sweden), and then detected by the ChemiDoc SRS image analysis system (Bio-Rad Laboratories).

Statistical analysis. Statistical analyses were performed with IBM SPSS Statistics for Windows, version 21.0 (IBM Corp., Armonk, NY, USA). P-values of <0.05 were considered to indicate a statistically significant difference. We used Dunnett's test for the time-dependent cell growth assay. Data are presented as means ± standard deviation.

Results

Determination of IC_{50} for CDDP and 17-AAG across a panel of ESCC cell lines. Treating esophageal cell lines with CDDP and 17-AAG resulted in dose-dependent cytotoxicity. Fig. 1 shows IC_{50} values for CDDP (Fig. 1A) and 17-AAG (Fig. 1B) across our panel of ESCC cell lines. IC_{50} values ranged from 0.983 to 14.9 μM for CDDP, and 0.0128 to 2.37 μM for 17-AAG, respectively. Based on these results, we decided to use KYSE30, KYSE150, EC-GI-10 and TE6 as representative CDDP-resistant cell lines in subsequent experiments.

CDDP and 17-AAG exhibit synergistic inhibitory effects on the growth of KYSE30 and KYSE150 esophageal squamous carcinoma cell lines. To evaluate the impact of the combined treatment with CDDP and 17-AAG on CDDP-resistant cell

Table I. Combination index value of the interaction between CDDP with 17-AAG against human esophageal carcinoma cell lines.

Cell line	IC_{50} of 17-AAG (μM)	Concentration of 17-AAG (μM)	CI at IC_{50}	Interpretation
KYSE30	2.37	1.000	0.49	Synergism
		0.500	0.76	Moderate synergism
KYSE150	0.10	0.050	0.71	Moderate synergism
		0.025	0.55	Synergism
EC-GI-10	1.40	1.000	1.80	Antagonism
		0.500	1.78	Antagonism
TE6	0.04	0.050	1.18	Moderate antagonism
		0.025	1.06	Additive effect

Different concentrations of 17-AAG were employed to study the effect on IC_{50} of CDDP. Variable ratios of drug concentrations and mutually non-exclusive equations were used to determine the CI. CI >1.3 indicates antagonism; CI = 1.1 to 1.3, moderate antagonism; CI = 0.9 to 1.1, additive effect; CI = 0.8 to 0.9, slight synergism; CI = 0.6 to 0.8, moderate synergism; CI = 0.4 to 0.6, synergism; and CI = 0.2 to 0.4, strong synergism. CI, combination index; CDDP, cisplatin.

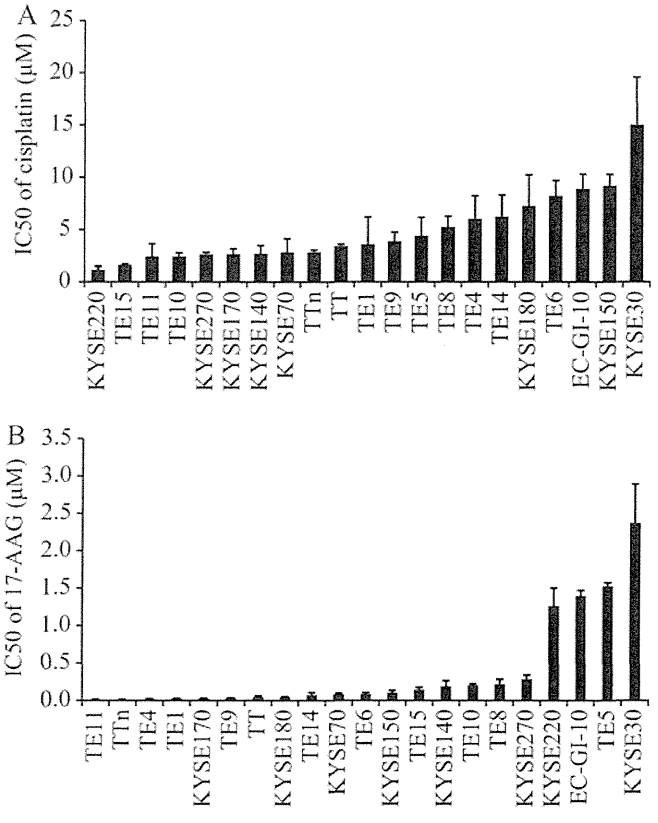

Figure 1. IC_{50} values for cisplatin (A) and 17-AAG (B) across the panel of esophageal squamous cell carcinoma cell lines. Cells were treated with a range of concentrations of cisplatin or 17-AAG for 72 h. Viable cell density was determined by a water-soluble tetrazolium salt and IC_{50} was calculated. The values and error bars represent the mean and standard deviation of at least three experiments performed in quintuplicate.

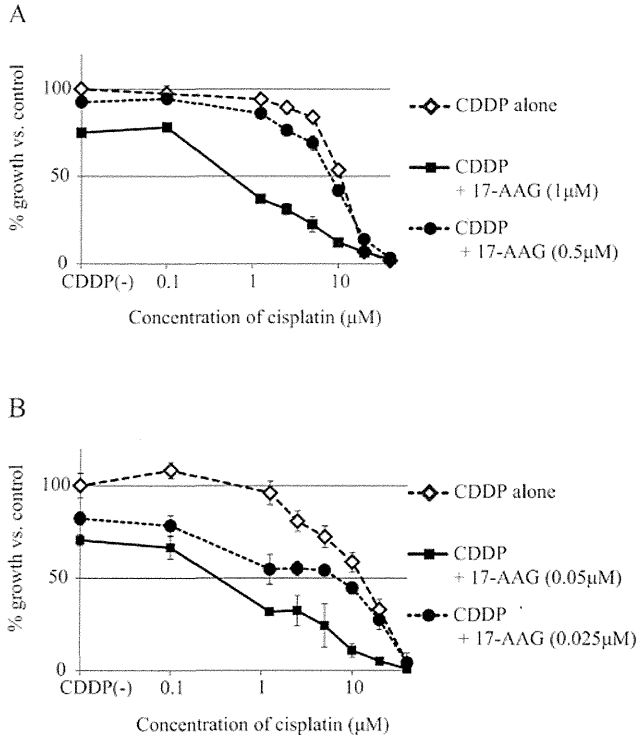

Figure 2. Dose-response curve for cisplatin (CDDP) in the presence of low doses of 17-AAG. KYSE30 and KYSE150 were treated with various doses of CDDP (0.1-40 μM) and 17-AAG (0.5-1 μM for KYSE30; 0.025-0.05 μM for KYSE150) for 72 h, and cytotoxicity was evaluated by a drug sensitivity assay. (A) KYSE30, (B) KYSE150. The experiment was performed twice and representative data are shown. Data are presented as means ± standard deviation of quintuplicate wells.

lines, KYSE30, KYSE150, EC-GI-10 and TE6 were treated with various concentrations of each drug alone or in combination, and were then subjected to a cell viability assay. As shown in Fig. 2, the combination with low-dose 17-AAG shifted the survival curve to the left in KYSE30 and KYSE150. The interaction between CDDP and 17-AAG was determined by calculating the CI. The CI values of KYSE30 and KYSE150 ranged from 0.4 to 0.7 for 50% cell kill, demonstrating synergistic behavior between CDDP and 17-AAG (Table I). In contrast, the CI value of EC-GI-10 and TE6 ranged from 1.0 to 1.8.

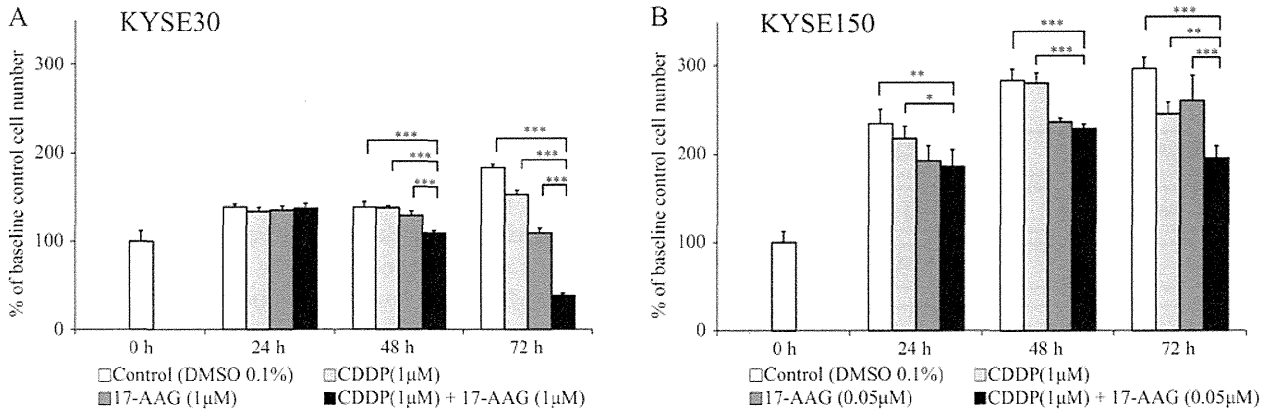

Figure 3. Changes in cell numbers by the treatment with cisplatin (CDDP) and 17-AAG, alone or in combination. (A) KYSE30 and (B) KYSE150 were exposed to 17-AAG alone (1 μM for KYSE30, 0.05 μM for KYSE150), CDDP alone (1 μM for both cell lines), and the combination of CDDP (1 μM for both cell lines) and 17-AAG (1 μM for KYSE30, 0.05 μM for KYSE150). Cell numbers were counted after 24, 48 and 72 h. Data are presented as means and standard deviation of quintuplicate wells. *P<0.05, **P<0.01, ***P<0.001.

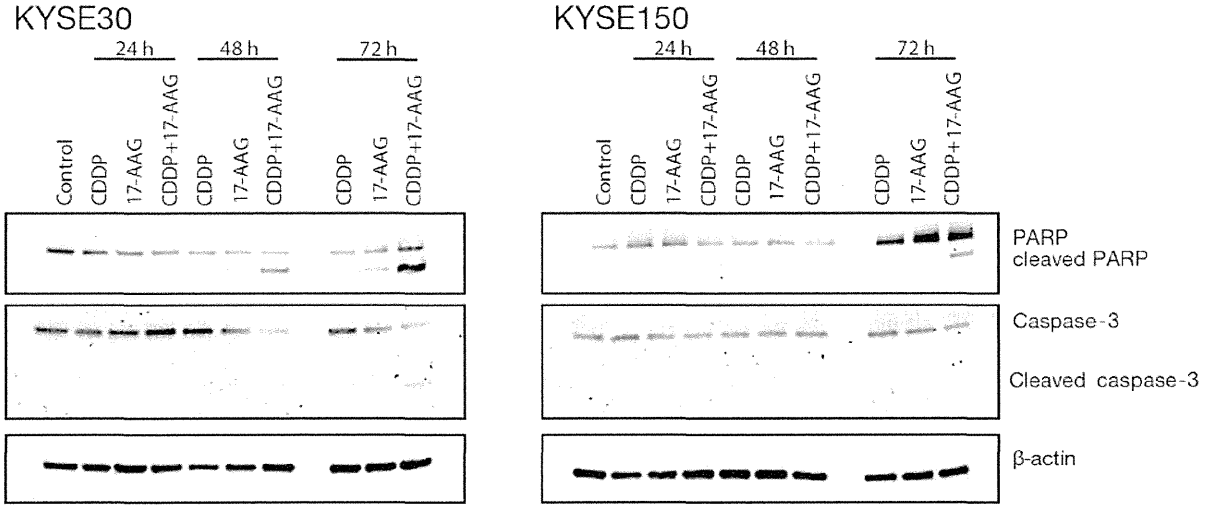

Figure 4. Induction of apoptosis by the combination of cisplatin (CDDP) and 17-AAG. KYSE30 was treated with CDDP (1 μM) and/or 17-AAG (1 μM), while KYSE150 was treated with CDDP (1 μM) and/or 17-AAG (0.05 μM). After the treatment, cell extracts were examined by western blot analysis.

These results showed either the additive or antagonistic effects of CDDP and 17-AAG in EC-GI-10 and TE6.

Cell count assay. To confirm the synergistic effect of CDDP and 17-AAG in KYSE30 and KYSE150, we counted actual cell numbers after treatment with the vehicle only (0.1% DMSO), 1 μM CDDP only, 1 μM 17-AAG only, and the combined treatment with 1 μM CDDP and 1 μM 17-AAG for 24, 48 and 72 h.

As shown in Fig. 3, low-dose CDDP alone and low-dose 17-AAG alone modestly suppressed cell growth in KYSE30 and KYSE150 (Fig. 3). However, the reduction in cell growth was significantly greater with the combination of CDDP and 17-AAG than with either drug alone.

Combination of CDDP and 17-AAG induces apoptosis. Using western blot analysis, we determined whether the reduced cell growth caused by the combined treatment with CDDP and 17-AAG occurred due to the induction of apoptosis via the cleavage of poly (ADP-ribose) polymerase (PARP) and activation of caspase-3.

No significant changes were observed in the expression of PARP and cleaved PARP 24 h after treatment with CDDP alone, 17-AAG alone, or CDDP and 17-AAG (Fig. 4). However, a clear increase was observed in cleaved PARP 48 h after the co-treatment with CDDP and 17-AAG in KYSE30 and KYSE150. The increase in cleaved PARP was greater than that with either drug alone. The induction of cleaved PARP was further enhanced at 72 h. Cleaved caspase-3 was detected 72 h after the co-treatment with CDDP and 17-AAG in KYSE30, but the band was weaker than that of cleaved PARP.

Combination of CDDP and 17-AAG reduces the expression of XIAP and phosphorylated Akt. To understand the mechanism underlying the synergy between CDDP and 17-AAG, we investigated the expression of proteins associated with apoptosis (Fig. 5). Under basal conditions, KYSE30 expressed high levels of XIAP, cIAP1, and survivin and low levels of cIAP2. KYSE150 expressed high levels of XIAP and cIAP1, and low levels of cIAP2 and survivin. Livin was not detected in either cell line.

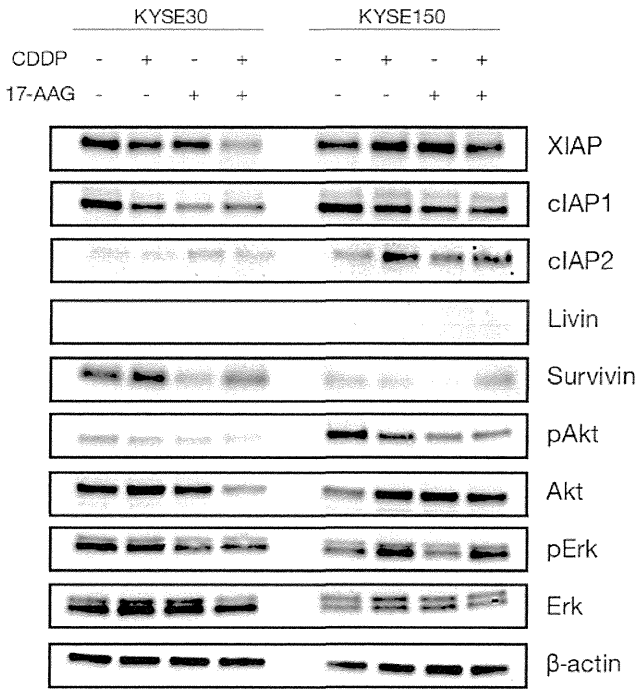

Figure 5. Western blot analysis of the IAP family proteins, the Erk and Akt pathways. KYSE30 and KYSE150 were treated with cisplatin (CDDP; 1 μM), 17-AAG (1 μM for KYSE30, 0.05 μM for KYSE150), and the combination of these drugs for 72 h, and cell lysates were analyzed by western blotting.

The treatment with CDDP alone, 17-AAG alone, or combined treatment with CDDP and 17-AAG induced variable changes in the levels of cIAP1, cIAP2 and survivin; however, a correlation was not observed between these changes and cell growth inhibition or the induction of apoptosis by the treatment. XIAP levels were, in contrast, unchanged by either agent alone, but were significantly reduced by the combined treatment. We also examined the expression of Bcl-2 family members, including Bcl-2, Bcl-xL, Bid, Bad, Bax, Bim, Beclin and BAG-1; however, no significant changes were observed by the treatment with CDDP alone, 17-AAG alone, or combined treatment with CDDP and 17-AAG (data not shown). These results demonstrated that the combination of CDDP and 17-AAG mainly induced apoptosis by inhibiting XIAP.

To identify the mechanism for the reduction in XIAP, the expression of the Akt and the Erk pathways was examined. As shown in Fig. 5, phosphorylated Akt levels were slightly reduced by either CDDP or 17-AAG alone in both cell lines. However, the combination of CDDP and 17-AAG clearly diminished phosphorylated Akt levels (Fig. 5). Phosphorylated Erk levels remained unchanged by the treatment in KYSE30. Phosphorylated Erk levels were modestly increased by CDDP alone and the combined treatment with CDDP and 17-AAG in KYSE150; however, no correlation was observed between these changes and the inhibition of cell growth or induction of apoptosis.

Time-dependent changes in the expression of phosphorylated Akt, total Akt, and XIAP. In order to determine time-dependent changes in phosphorylated Akt, total Akt and XIAP, we examined the expression of these proteins after the treatment with CDDP and/or 17-AAG, either alone or in combination (Fig. 6). Phosphorylated Akt levels were modestly reduced by 17-AAG alone and by the combination of CDDP and 17-AAG after 24 h. Further reductions occurred at 72 h, especially with the combination of CDDP and 17-AAG in KYSE30. The expression of phosphorylated Akt was not significantly changed by CDDP alone. The expression of XIAP was reduced by 17-AAG alone and by the combination of CDDP and 17-AAG, similar to that for phosphorylated Akt.

Discussion

In the present study, we demonstrated that the combined treatment with CDDP and 17-AAG had synergistic inhibitory effects on cell growth in CDDP-resistant ESCCs. The synergistic interaction between CDDP and 17-AAG resulted in significant increases in the cytotoxicity of CDDP; a strong cytotoxic effect was obtained in the presence of low-dose 17-AAG, which hardly has a cytotoxic effect by itself, in combination with a low concentration of CDDP. This cytotoxic effect occurred via induction of apoptosis, as demonstrated by the cleavage of PARP and caspase-3.

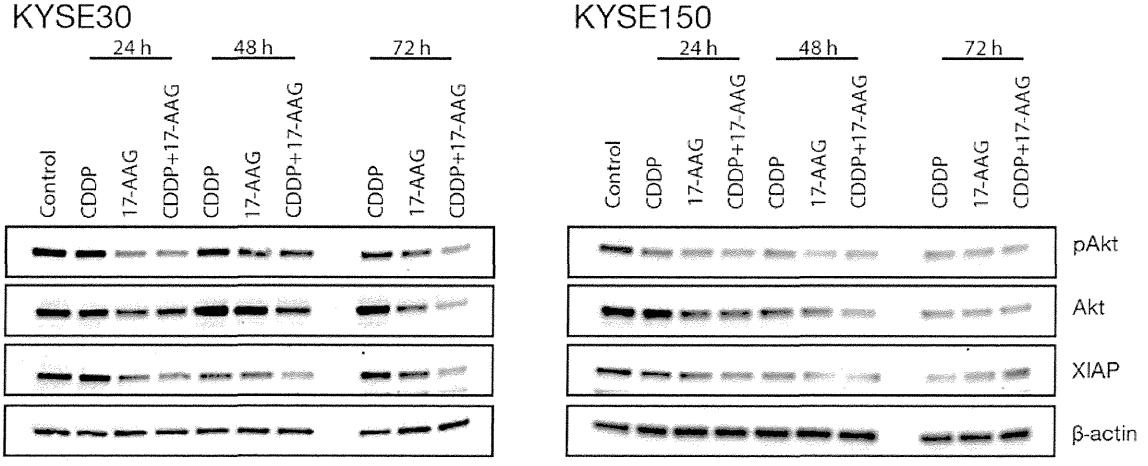

Figure 6. Time-dependent changes in the expression of phosphorylated Akt, Akt and XIAP. KYSE30 and KYSE150 were treated with cisplatin (CDDP; 1 μM), 17-AAG (1 μM for KYSE30, 0.05 μM for KYSE150), and the combination of these drugs for the indicated times, and cell lysates were analyzed by western blotting.

The synergy between CDDP and an HSP90 inhibitor has been reported in previous studies; for example, McCollum *et al* reported that CDDP was synergistic with geldanamycin or 17-AAG and combined treatment with the two drugs increased apoptosis in the lung cancer cell line A549 (12). This synergy was attributed in part to the CDDP-induced abrogation of heat shock factor-1 activity. Weng *et al* also showed that 17-AAG enhanced CDDP cytotoxicity in the non-small cell lung cancer cell lines, A549 and H1650 (13). This synergistic effect was reported to be mediated by the downregulation of thymidine phosphorylase and Akt activation. We have yet to examine whether similar mechanisms occur in our cell lines. Nevertheless, our study provides the first evidence for the synergy of CDDP and 17-AAG in CDDP-resistant esophageal squamous cell lines.

We also revealed that, among the major regulators of apoptosis, the Akt/XIAP pathway mediated the synergistic effect of CDDP and 17-AAG; the expression patterns of phosphorylated Akt and XIAP levels closely correlated with their inhibitory effect on cell growth, induction of PARP cleavage, and apoptosis, which occurred by the combined treatment with CDDP and 17-AAG. Moreover, time-course experiments demonstrated that the reduction in phosphorylated Akt and XIAP levels were concomitant with the induction of PARP cleavage and apoptosis.

Previous studies indicated the Akt/XIAP pathway as the main regulator of apoptosis by chemotherapy in some cancer cell lines, including carcinomas of the breast, ovary, uterine cervix and melanoma (14-17). Akt phosphorylates and stabilizes XIAP, and the deactivation or knockdown of Akt destabilizes XIAP, leading to apoptosis (18). In addition, specific inhibition of XIAP expression was shown to induce apoptosis and increase caspase-3 activity in prostate cancer cells (19). These findings support our conclusion that the synergistic effect of CDDP and 17-AAG is mediated by the induction of apoptosis via the Akt and XIAP pathways.

One limitation of our study is that we lack data showing the synergy of CDDP and 17-AAG *in vivo*, and such data will be required to extrapolate the current results to clinical situations. We also cannot explain why synergy occurred in KYSE30 and KYSE150, but not in EC-GI-10 or TE6. A recent study indicated phosphatase and tensin homolog (PTEN) as a potential predictive marker for HSP90 inhibitor sensitivity among four ESCC cell lines (20). However, biomarkers that predict the HSP90 response or synergy of an HSP90 inhibitor and CDDP have not yet been established (21). The identification of such biomarkers is crucial in clinical settings.

In conclusion, we showed that the combination of low concentrations of CDDP with low-dose 17-AAG exerted synergistic effects on CDDP-resistant ESCC cell lines. The mechanism of the synergy was attributed to apoptosis mediated by downregulation of the Akt/XIAP pathway. Our results indicate that the co-administration of low-dose 17-AAG and CDDP overcomes CDDP chemoresistance and may improve the outcomes of patients with ESCC.

References

1. Jemal A, Bray F, Center MM, Ferlay J, Ward E and Forman D: Global cancer statistics. CA Cancer J Clin 61: 69-90, 2011.
2. Ozawa S, Tachimori Y, Baba H, *et al*: Comprehensive registry of esophageal cancer in Japan, 2004. Esophagus 9: 75-98, 2012.
3. Miyata H, Yamasaki M, Kurokawa Y, *et al*: Multimodal treatment for resectable esophageal cancer. Gen Thorac Cardiovasc Surg 59: 461-466, 2011.
4. Berrino F, De Angelis R, Sant M, *et al*: Survival for eight major cancers and all cancers combined for European adults diagnosed in 1995-99: results of the EUROCARE-4 study. Lancet Oncol 8: 773-783, 2007.
5. Siegel R, Naishadham D and Jemal A: Cancer statistics, 2012. CA Cancer J Clin 62: 10-29, 2012.
6. Yamasaki M, Miyata H, Tanaka K, *et al*: Multicenter phase I/II study of docetaxel, cisplatin and fluorouracil combination chemotherapy in patients with advanced or recurrent squamous cell carcinoma of the esophagus. Oncology 80: 307-313, 2011.
7. Hara H, Tahara M, Daiko H, *et al*: Phase II feasibility study of preoperative chemotherapy with docetaxel, cisplatin, and fluorouracil for esophageal squamous cell carcinoma. Cancer Sci: Aug 30, 2013 (Epub ahead of print).
8. Neckers L and Neckers K: Heat-shock protein 90 inhibitors as novel cancer chemotherapeutic agents. Expert Opin Emerg Drugs 7: 277-288, 2002.
9. Newman B, Liu Y, Lee HF, Sun DX and Wang Y: HSP90 inhibitor 17-AAG selectively eradicates lymphoma stem cells. Cancer Res 72: 4551-4561, 2012.
10. Zhang H and Burrows F: Targeting multiple signal transduction pathways through inhibition of Hsp90. J Mol Med 82: 488-499, 2004.
11. Chou TC: Theoretical basis, experimental design, and computerized simulation of synergism and antagonism in drug combination studies. Pharmacol Rev 58: 621-681, 2006.
12. McCollum AK, Lukasiewicz KB, Teneyck CJ, Lingle WL, Toft DO and Erlichman C: Cisplatin abrogates the geldanamycin-induced heat shock response. Mol Cancer Ther 7: 3256-3264, 2008.
13. Weng SH, Tseng SC, Huang YC, Chen HJ and Lin YW: Inhibition of thymidine phosphorylase expression by using an HSP90 inhibitor potentiates the cytotoxic effect of cisplatin in non-small-cell lung cancer cells. Biochem Pharmacol 84: 126-136, 2012.
14. Pramanik KC, Kudugunti SK, Fofaria NM, Moridani MY and Srivastava SK: Caffeic acid phenethyl ester suppresses melanoma tumor growth by inhibiting PI3K/AKT/XIAP pathway. Carcinogenesis 34: 2061-2070, 2013.
15. Rajput S, Kumar BN, Sarkar S, *et al*: Targeted apoptotic effects of thymoquinone and tamoxifen on XIAP mediated Akt regulation in breast cancer. PLoS One 8: e61342, 2013.
16. Gagnon V, Van Themsche C, Turner S, Leblanc V and Asselin E: Akt and XIAP regulate the sensitivity of human uterine cancer cells to cisplatin, doxorubicin and taxol. Apoptosis 13: 259-271, 2008.
17. Asselin E, Mills GB and Tsang BK: XIAP regulates Akt activity and caspase-3-dependent cleavage during cisplatin-induced apoptosis in human ovarian epithelial cancer cells. Cancer Res 61: 1862-1868, 2001.
18. Dan HC, Sun M, Kaneko S, *et al*: Akt phosphorylation and stabilization of X-linked inhibitor of apoptosis protein (XIAP). J Biol Chem 279: 5405-5412, 2004.
19. Amantana A, London CA, Iversen PL and Devi GR: X-linked inhibitor of apoptosis protein inhibition induces apoptosis and enhances chemotherapy sensitivity in human prostate cancer cells. Mol Cancer Ther 3: 699-707, 2004.
20. Bao XH, Takaoka M, Hao HF, *et al*: Antiproliferative effect of the HSP90 inhibitor NVP-AUY922 is determined by the expression of PTEN in esophageal cancer. Oncol Rep 29: 45-50, 2013.
21. Garcia-Carbonero R, Carnero A and Paz-Ares L: Inhibition of HSP90 molecular chaperones: moving into the clinic. Lancet Oncol 14: e358-e369, 2013.

Laboratory Investigation (2013) 93, 1137–1146
© 2013 USCAP, Inc All rights reserved 0023-6837/13

Enhanced autophagy is required for survival in EGFR-independent *EGFR*-mutant lung adenocarcinoma cells

Yuji Sakuma[1,2,5], Shoichi Matsukuma[1], Yoshiyasu Nakamura[1], Mitsuyo Yoshihara[1], Shiro Koizume[1], Hironobu Sekiguchi[2], Haruhiro Saito[3], Haruhiko Nakayama[3], Yoichi Kameda[4], Tomoyuki Yokose[4], Sachiko Oguni[5], Toshiro Niki[5] and Yohei Miyagi[1,2]

Lung cancers harboring epidermal growth factor receptor (*EGFR*) mutations depend on constitutive activation of the kinase for survival. Although most *EGFR*-mutant lung cancers are sensitive to EGFR tyrosine kinase inhibitors (TKIs) and shrink in response to treatment, acquired resistance to TKI therapy is common. We demonstrate here that two *EGFR*-mutated lung adenocarcinoma cell lines, HCC827 and HCC4006, contain a subpopulation of cells that have undergone epithelial-to-mesenchymal transition and survive independent of activated EGFR. These EGFR-independent cancer cells, herein termed gefitinib-resistant (GR) cells, demonstrate higher levels of basal autophagy than their parental cells and thrive under hypoxic, reduced-serum conditions *in vitro*; this somewhat simulates the hypoxic environment common to cancerous tissues. We show that depletion of the essential autophagy gene, *ATG5*, by small interfering RNA (siRNA) or chloroquine, an autophagy inhibitor, markedly reduces GR cell viability under hypoxic conditions. Moreover, we show a significant elevation in caspase activity in GR cells following knockdown of ATG5. These results suggest that GR cells can evade apoptosis and survive in hostile, hypoxic environments with constant autophagic flux. We also show the presence of autophagosomes in some cancer cells from patient samples, even in untreated *EGFR*-mutant lung cancer tissue samples. Together, our results indicate that autophagy inhibitors alone or in combination with EGFR TKIs may be an effective approach for the treatment of *EGFR*-mutant lung cancers, where basal autophagy of some cancer cells is upregulated.

Laboratory Investigation (2013) **93,** 1137–1146; doi:10.1038/labinvest.2013.102; published online 12 August 2013

KEYWORDS: acquired resistance; autophagy; *EGFR* mutation; epithelial-to-mesenchymal transition (EMT); lung adenocarcinoma

Activating mutations in the epidermal growth factor receptor (*EGFR*) gene are critical for the growth and survival of lung cancers. EGFR tyrosine kinase inhibitors (TKIs), such as gefitinib or erlotinib, have been shown to be effective against tumor growth during the initial stages of treatment in these cancer subtypes. However, *EGFR*-mutated tumors invariably acquire resistance to these EGFR TKIs, most commonly through a spontaneous secondary mutation (T790M) in *EGFR*, or via the amplification or ligand-dependent stimulation of Met kinase.[1,2] Several therapeutic options to treat these resistant tumors have been developed, including WZ4002, a third-generation EGFR TKI that can effectively inhibit the kinase activity of T790M-mutated EGFR.[3] In addition, combinatorial treatment with TKIs against both EGFR and Met can induce apoptosis in Met-activated *EGFR*-mutated cancer cells.[4] *EGFR*-mutated tumors can also acquire resistance to EGFR TKIs through epithelial-to-mesenchymal transition (EMT).[5–8] Furthermore, the AXL receptor tyrosine kinase has been shown to have a key role in EMT-induced drug resistance;[9] however, it remains unclear whether AXL activation invariably occurs in *EGFR*-mutant carcinoma cells showing an EMT phenotype.

Autophagy describes the process by which cells capture intracellular proteins, lipids, and organelles into autophagosomes, and deliver them to the lysosomes to form autophagolysosomes (also termed autolysosomes) for degradation. These degradation products are then exported from autophagolysosomes into the cytoplasm for recycling.

[1]Molecular Pathology and Genetics Division, Kanagawa Cancer Center Research Institute, Yokohama, Japan; [2]Laboratory for Molecular Diagnostics, Kanagawa Cancer Center Hospital, Yokohama, Japan; [3]Department of Thoracic Oncology, Kanagawa Cancer Center Hospital, Yokohama, Japan; [4]Department of Pathology, Kanagawa Cancer Center Hospital, Yokohama, Japan and [5]Department of Pathology, Jichi Medical University, Tochigi, Japan
Correspondence: Dr Y Sakuma, MD, PhD, Department of Pathology, Jichi Medical University, 3311-1 Yakushiji, Shimotsuke, Tochigi 329-0498, Japan.
E-mail: ysakuma@jichi.ac.jp

Received 30 May 2013; revised 26 July 2013; accepted 26 July 2013

This intracellular recycling function maintains both normal cells and cancer cells in a healthy state, and thereby promotes the survival of malignant cells once the tumor is established. The core molecular machinery required for the formation of an autophagosome comprises a heterogeneous group of proteins encoded by autophagy-related *ATG* genes, such as ATG5, Beclin1 (also known as ATG6), and microtubule-associated protein 1 light chain 3 (LC3), a human homolog of yeast ATG8.[10–12] The conversion of cytosolic LC3-I to autophagosome-bound LC3-II acts as a biochemical marker of active autophagy,[10–16] and it has been increasingly appreciated that the immunohistochemical detection of cytoplasmic LC3 puncta in formalin-fixed, paraffin-embedded specimens (FFPE) correlates with the amount of autophagosomes or autophagolysosomes.[14,17,18] Although it is known that cancer cells with *Ras* mutations are addicted to upregulated autophagic flux,[10,11,13,14] little has been done to clarify the role of autophagy in *EGFR*-driven carcinoma cells.[19,20]

In this study, we demonstrate that gefitinib-resistant (GR) *EGFR*-mutant lung carcinoma cells with an EMT phenotype can survive under hypoxic conditions *in vitro* in the absence of *EGFR* T790M mutation or Met, EGFR, or AXL activity because of enhanced autophagic flux. Furthermore, using immunohistochemistry and electron microscopy, we also demonstrate cytoplasmic, granular expression of LC3A (an isoform of LC3) in untreated *EGFR*-mutant lung cancer tissues, as well as the formation of autophagosomes in these cells.

MATERIALS AND METHODS

The experimental procedures were approved by the Institutional Review Board at the Kanagawa Cancer Center, Japan.

Cell Culture and Drugs

Two *EGFR*-mutant lung adenocarcinoma cell lines, HCC827 (del E746-A750) and HCC4006 (del L747-E749 + A750P), were purchased from the American Type Culture Collection (Manassas, VA, USA) and maintained in RPMI1640 media containing 10% fetal calf serum (FCS) and antibiotics at 37 °C in a humidified incubator with 20% O_2 + 5% CO_2. A cancer tissue microenvironment was simulated with RPMI1640 media containing 1% FCS and antibiotics at 37 °C in a humidified incubator with 1% O_2 + 5% CO_2. Two EGFR TKIs, gefitinib (Biaffin GmbH & Co KG, Kassel, Germany) and WZ4002 (Selleck Chemicals, Houston, TX, USA), were used in this study, as well as an autophagy-inducing drug, salinomycin (Sigma-Aldrich, St Louis, MO, USA)[21] and a late-stage inhibitor of autophagy, chloroquine (CQ) diphosphate salt (Sigma-Aldrich).[11]

Generation of GR HCC827 and HCC4006 Cells

HCC827 and HCC4006 cells were cultured in the presence of 1 μM gefitinib until they acquired resistance. After surviving 20 passages in the presence of the drug, single-cell cloning was performed using cloning cylinders. GR subclones were successfully expanded in media containing 1 μM gefitinib and were termed HCC827 GR1–5 or HCC4006 GR1–3 cells, respectively. HCC827 GR2 and HCC4006 GR3 sublines are characterized in detail in this study.

Loop-hybrid Mobility Shift Assay

A loop-hybrid mobility shift assay (LH-MSA) was used for the detection of T790M mutation in *EGFR*.[22–24] Briefly, cell-derived DNA was subjected to PCR with a primer pair (5′-ctccaccgtgcaagctcatca-3′ and 5′-gtactgggagccaatattgtctttg-3′) and then a Cy5-labeled LH probe was added to the product at a final concentration of 240 nM (Cy5-5′-ctccaccgtgcaagctcatcacATATATATAgcagctcatgcccttcggctgcc-3′; insertion is denoted by capital letters) using a hybridization procedure of 94 °C for 2 min, 55 °C for 45 s, and 68 °C for 4 min. The reacted products were separated by 10% polyacrylamide gel electrophoresis (C10L; Atto Inc, Tokyo, Japan) and detected with STORM860 (GE Healthcare, Buckinghamshire, UK) for Cy5 fluorescence (at 635 nm with an LP650 filter).

RNA Interference Assay

Cells (20×10^5) were plated in 94-mm culture dishes, grown for 24 h, and then transfected with siRNA duplexes targeting EGFR (SI02663983), AXL (SI00605311), or ATG5 (SI02655310), and with negative control siRNA duplexes (1027281) (Qiagen, Valencia, CA, USA) using Lipofectamine RNAiMAX Reagent and OPTI-MEM I (Invitrogen), according to the manufacturer's recommendations.

Quantitative RT-PCR

Total RNA was extracted with the RNeasy Mini Kit (Qiagen) and 1 μg RNA was reverse transcribed into cDNA using the QuantiTect Reverse Transcription Kit (Qiagen). Real-time PCR was performed using the QuantiTect Primer Assay and QuantiFast SYBR Green PCR Kit (Qiagen) in a LightCycler 480 (Roche Applied Science, Mannheim, Germany). β-actin mRNA (Hs_ACTB_2_SG) was used to standardize the quantity of LC3A mRNA (Hs_MAP1LC3A_1_SG). The relative expression of LC3A mRNA between parental cells and GR cells was calculated by the difference in the threshold cycle (comparative C_T method). Data are presented as the mean ± s.d. of triplicate experiments.

Western Blotting

Western blotting for the expression of poly(ADP-ribose) polymerase-1 (PARP-1), total EGFR, phosphorylated EGFR (pEGFR), γH2AX, and β-actin was performed as described previously.[25,26] Additional primary antibodies for immunoblotting were anti-E-cadherin (34; 1:500 dilution; BD Biosciences, Franklin Lakes, NJ, USA), anti-Ep-CAM (C-10; 1:1000 dilution; Santa Cruz Biotechnology, Santa Cruz, CA, USA), anti-Vimentin (SP20; 1:2000 dilution; Epitomics, Burlingame, CA, USA), anti-Met (C-12; 1:2000

dilution; Santa Cruz Biotechnology), anti-CD44 (EPR1031Y; 1:2000 dilution; Epitomics), anti-AXL (C44G1; 1:1000 dilution; Cell Signaling, Tokyo, Japan), anti-LC3A (D50G8; 1:1000 dilution; Cell Signaling), anti-ATG5 (D5G3; 1:1000 dilution; Cell Signaling), and anti-Beclin1 (D40C5; 1:1000 dilution; Cell Signaling). Band intensity levels on X-ray films were normalized to β-actin using Image J software (NIH, Bethesda, MD, USA). Each experiment was performed in triplicate.

Assessment of Cell Viability and Apoptosis

Cell viability was assessed by trypan blue exclusion or using a WST-1 assay (Roche Applied Science). Apoptosis was assessed by western blot analysis of the cleaved PARP-1 or Caspase-Glo 3/7 Assay (Promega, Madison, WI, USA), as previously described.[25,26]

Primary *EGFR*-Mutant Lung Cancer Tissues

Tumor samples were obtained from 20 *EGFR*-mutant lung cancer patients who underwent surgery at the Kanagawa Cancer Center Hospital between August 2002 and August 2007. The patients included 10 men and 10 women, with a median age of 58.5 years (range 38–80 years). Aside from one patient (adenosquamous cell carcinoma), all tumors were classified as adenocarcinoma by histology. *EGFR* mutations were identified as a deletion mutation in exon 19 ($n=11$) or an L858R point mutation in exon 21 ($n=9$). None of the patients received neoadjuvant chemotherapy before surgery.

Immunohistochemistry

Immunohistochemical staining for LC3A was performed on FFPE tissue sections of lung cancers. Tissue sections were retrieved by autoclave treatment (121 °C for 15 min) in a citrate buffer (pH 6.0). Slides were then incubated overnight at 4 °C with anti-LC3A (1:3200 dilution). Immunohistochemical staining of peripheral nerve bundles in the tissue was used as an internal positive control.[14,17] The cancer tissue was judged as positive for LC3A expression when 5% or more carcinoma cells stained positive for LC3A.

Transmission Electron Microscopy

Ultrastructural studies were performed using an FFPE tissue sample obtained from one patient whose tumor showed highest positivity for LC3A expression by immunohistochemistry. The tissue was deparaffinized and then re-fixed in 2.5% glutaraldehyde overnight at 4 °C. After post fixation in 1% osmium tetroxide for 1 h and dehydration, the sample was embedded in epon. Conventional thin sections were collected on uncoated grids, stained with uranyl acetate and lead citrate, and then examined with a JEM-1400Plus transmission electron microscope (JEOL, Tokyo, Japan).

Statistical Analysis

Differences in caspase activity or cell viability between untreated and treated cells were evaluated by paired *t*-tests. Differences in the expression levels of total EGFR or pEGFR, expression levels of LC3A mRNA, and cell viability between parental cells and GR cells were evaluated by unpaired *t*-tests. *P*-values <0.05 were considered significant. All statistical calculations were performed with the JMP software (JMP for Windows version 7; SAS Institute Japan; Tokyo, Japan).

RESULTS

GR Cells Display an EMT Phenotype in the Absence of *EGFR* T790M Mutation or Met Activation

We first confirmed that HCC827 GR2 and HCC4006 GR3 cells had the same deletion mutation in *EGFR* as their respective parental cells, and that neither GR cell line carried the T790M mutation by LH-MSA and sequencing (Figure 1a and data not shown). In addition, Met expression in GR cells was considerably lower than that in the parental cells (Figure 1b). Combinatorial therapy with gefitinib and PHA665752, a Met TKI, did not induce apoptosis in GR cells (data not shown), indicating that these GR cells do not require Met activation for survival. These findings indicate that both HCC827 GR2 and HCC4006 GR3 cells lack the two recognized molecular mechanisms that confer resistance to EGFR TKI therapy.

Following this, we used western blot analysis to show that two epithelial markers, E-cadherin and Ep-CAM, were markedly downregulated in GR cells as compared with the parental cells, and that the mesenchymal marker vimentin was substantially elevated in GR cells (Figure 1b). Using light microscopy, we observed that GR cells were spindle shaped but the parental cells had a cobblestone-like appearance (Figure 1c and data not shown). These findings provided evidence for the EMT phenotype of GR cells. We also observed a marked increase in CD44 expression in GR cells as compared with their parental cells (Figure 1b). As parental HCC827 and HCC4006 cell lines contain a minor subpopulation of cells that express CD44 ($<1\%$),[5] it is likely that gefitinib treatment selected for these pre-existing GR cells from the parental cell culture.

Interestingly, in HCC827 GR2 cells, we observed a marked decrease in the expression of pEGFR relative to the parental cells, but no change in total EGFR expression (Figure 1d). By comparison, although pEGFR was also significantly reduced in HCC4006 GR3 cells as compared with parental cells, there was a similar significant reduction in total EGFR levels in these cells (Figure 1e). This marked decrease in EGFR kinase activity suggests that GR cells are less dependent on EGFR signaling for survival than the parental cells.

GR Cells do not Depend on EGFR Signaling for Survival

To confirm the hypothesis that GR cells are not dependent on EGFR signaling, we sought to examine changes in the expression of several cell death markers between GR and their

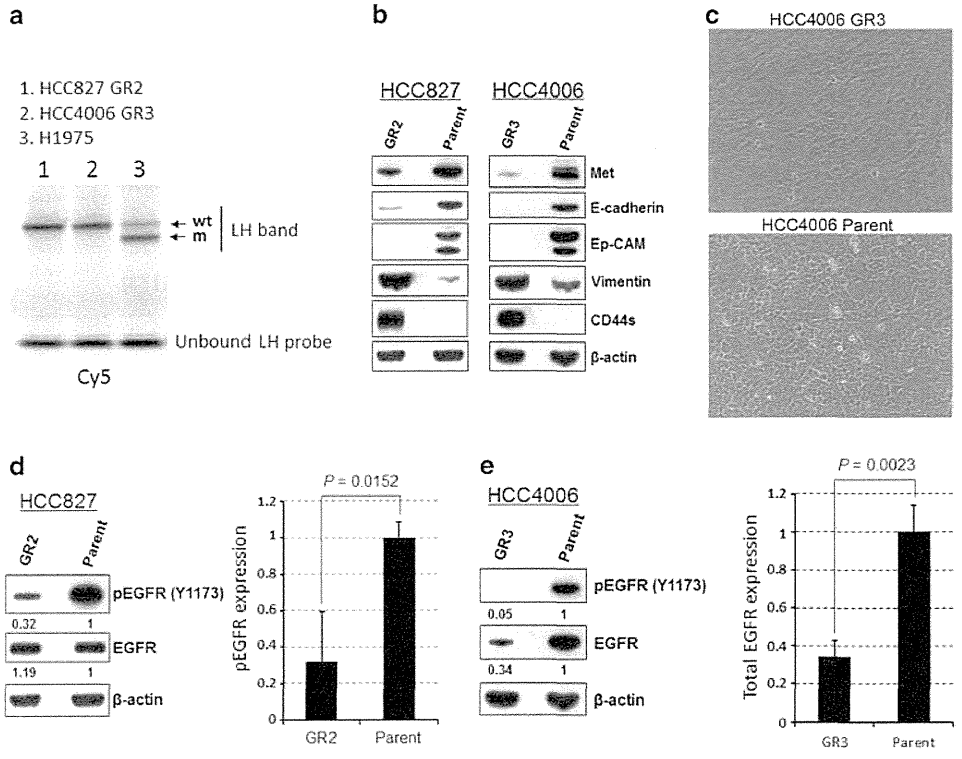

Figure 1 Gefitinib-resistant (GR) cells displayed an epithelial-to-mesenchymal transitioned (EMT) phenotype. (**a**) Detection of epidermal growth factor receptor (*EGFR*) T790M mutation by the loop-hybrid mobility shift assay (LH-MSA). Representative heterozygous LH band patterns of the wild-type (wt) and the T790M mutation (m) after LH-MSA using an LH probe are illustrated. The mutation is present in H1975 cells (an *EGFR*-mutant cell line having the T790M mutation), but not HCC827 GR2 or HCC4006 GR3 cells. (**b**) Western blots of HCC827 or HCC4006 GR and their respective parental cells. CD44s, standard isoform of CD44. (**c**) Representative phase-contrast images of HCC4006 GR3 cells and parental cells. (**d**, **e**) (Left panel) Western blots of (**d**) HCC827 GR2 and parental cells and (**e**) HCC4006 GR3 and parental cells. The expression levels of phosphorylated EGFR (pEGFR) and total EGFR were normalized to β-actin. (Right panel) Quantification of (**d**) pEGFR expression and (**e**) total EGFR expression. Results are expressed as the mean ($n = 3$) and s.d.

parental cells after EGFR TKI treatment. In parental HCC827 and HCC4006 cells, EGFR autophosphorylation was suppressed with gefitinib or WZ4002, and the cells clearly underwent apoptosis, with an increased expression of γH2AX (a DNA damage marker), a significant elevation in caspase 3/7 activity, and cleavage of PARP-1 (Figure 2a and b). However, these markers remained unchanged in GR cells in the presence of EGFR TKIs (Figures 2a and b). In addition, siRNA-mediated EGFR knockdown also did not induce apoptosis in both GR cell lines (Figure 2c). These results confirmed our hypothesis that GR cells do not depend on EGFR signaling for survival, despite the presence of the same activating mutations in *EGFR* as their parental cells. Both gefitinib and WZ4002 almost completely suppressed EGFR autophosphorylation in HCC827 GR2 cells, as well as its parental cells (Figure 2a). Further, total EGFR was upregulated in HCC4006 GR3 cells following treatment with EGFR TKIs (Figure 2a), suggesting that activated drug efflux was not responsible for the GR cells' resistance to EGFR TKIs. These responses to gefitinib treatment observed in both GR cells also support the absence of EGFR T790M mutation in GR cells, because gefitinib cannot suppress the kinase activity nor affect the expression levels of mutant EGFR with the T790M mutation.[2,3]

AXL Kinase does not have a Critical Role in GR Cell Survival

Because AXL kinase has been shown to have a key role in EMT-induced drug resistance, we sought to rule out its involvement in GR cells. HCC4006 GR3 cells showed a higher expression of AXL kinase than the parental cells. Comparatively, AXL expression in HCC827 GR2 cells was too low for detection, with only faint protein expression observed in the parental cells (Figure 3a). In HCC4006 GR3 cells, siRNA-mediated AXL knockdown followed by gefitinib treatment had no effect on γH2AX or PARP-1 cleavage (Figure 3b). As expected, HCC827 GR2 cells were insensitive to the same treatment (data not shown). These results indicate that GR cells do not require AXL kinase activity for survival.

GR Cells have Higher Levels of Basal Autophagy than Parental Cells

Next, we sought to test the role of autophagy in GR cells using autophagosome-bound LC3A-II as a biochemical

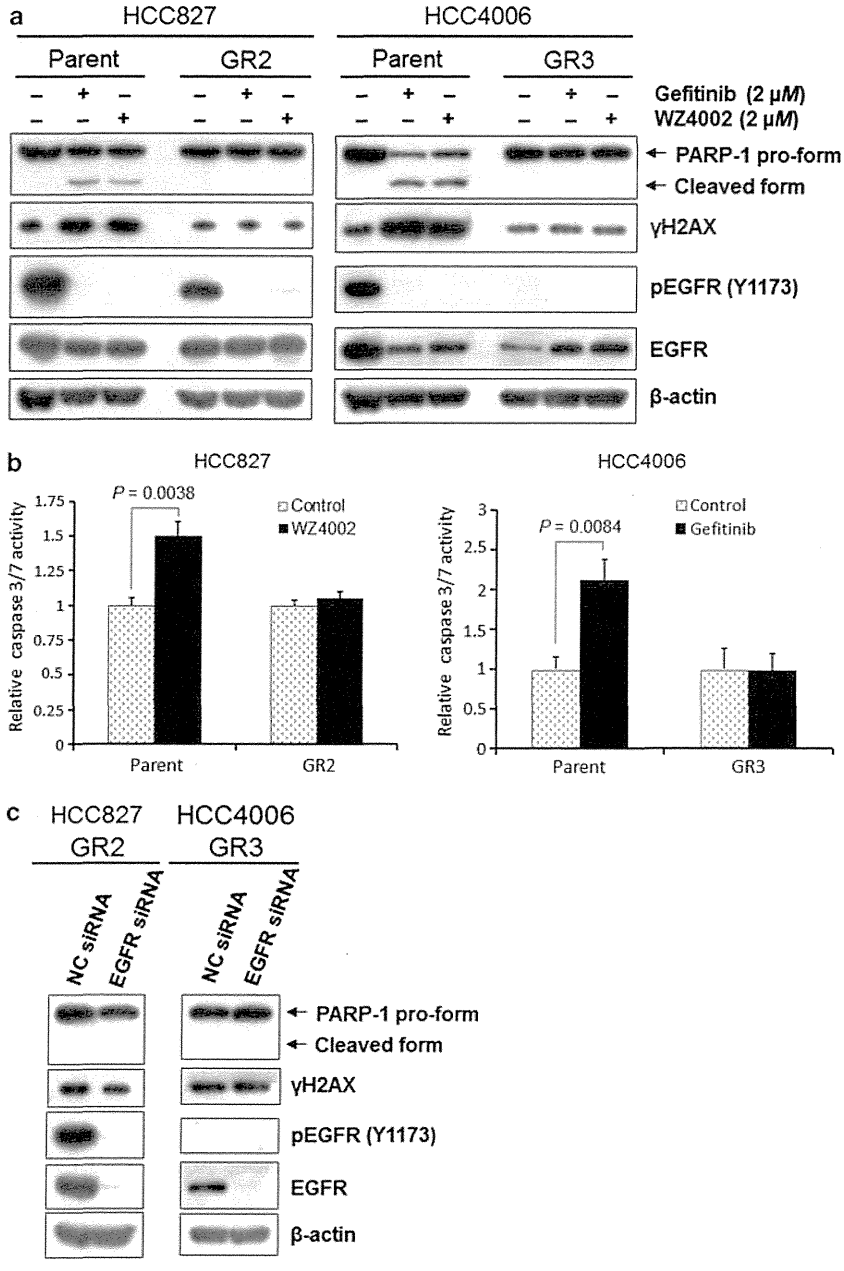

Figure 2 Gefitinib-resistant (GR) cells do not depend on epidermal growth factor receptor (EGFR) activity for survival. (**a**) Western blots examining the effects of gefitinib or WZ4002 treatment on apoptosis in parental cells and GR cells. Cells were untreated or treated with the indicated drug for 48 h. (**b**) Caspase 3/7 activity in HCC827 and HCC4006 cells. Cells were untreated or treated with the indicated drug (2 μM) for 24 h. Caspase activity was normalized to an arbitrary unit of 1.0 for the mean of three untreated wells. Results are expressed as the mean ($n = 3$) and s.d. (**c**) Western blots examining the effects of EGFR depletion on apoptosis in HCC827 GR2 and HCC4006 GR3 cells. Cells were transfected with negative control (NC) small interfering RNA (siRNA) or EGFR siRNA, and cultured for 72 h.

marker of active autophagy. GR cells cultured in 20% oxygen and 10% FCS (hereafter called 'normoxic conditions') had a much higher expression of LC3A mRNA and autophagosome-bound LC3A-II protein as compared with those levels in the parental cells (Figures 4a–c). This was true even when GR and their parental cells were treated by salinomycin, an autophagy-inducing drug,[21] or CQ, a late-stage inhibitor of autophagy.[11] These findings indicate that GR cells have significantly higher levels of basal autophagy than their respective parental cells. Although both parental cells were able to grow in the presence of CQ, HCC827 GR2 cells treated with CQ showed minimal proliferation, and HCC4006 GR3 cell viability was decreased (Figure 4d). These results suggest that GR cells are more dependent on autophagic flux for survival or proliferation than their parental cells, even under normoxic conditions. GR cells showed

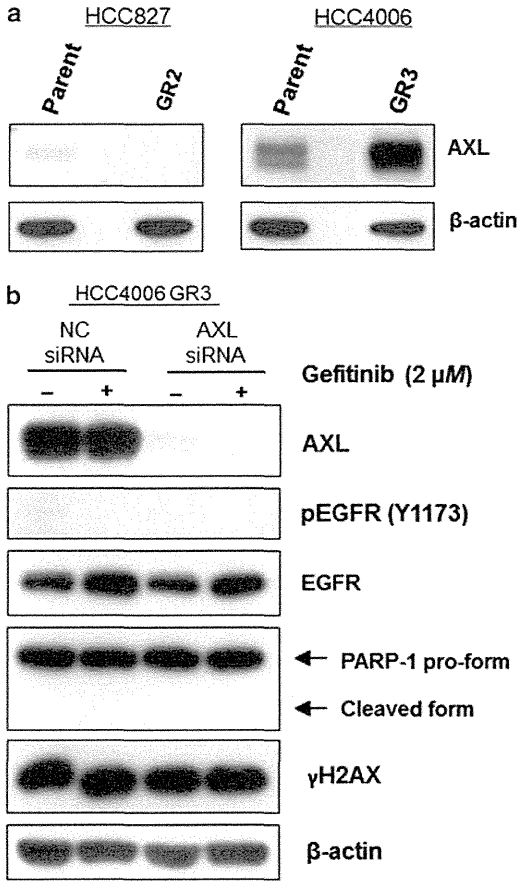

Figure 3 Gefitinib-resistant (GR) cells can survive independently of AXL receptor tyrosine kinase. (**a**) Western blots of HCC827 or HCC4006 parental and GR cells for the AXL kinase. (**b**) Western blots examining the effects of AXL depletion, gefitinib treatment, or a combination of AXL depletion and gefitinib or neither in HCC4006 GR3 cells. Cells transfected with negative control (NC) small interfering RNA (siRNA; 10 nM) or AXL-specific siRNA (10 nM) were cultured for 72 h and then untreated or treated with gefitinib (2 μM) for another 48 h.

slightly decreased expression of ATG5 as compared with their parental cells, and both GR cells and parental cells expressed Beclin1 in almost equal amounts (Figures 4b and c).

High Basal Autophagy Promotes Survival of GR Cells Under Hypoxia

Autophagy in cancer cells and EMT are both known to be induced in hypoxic microenvironments,[10,11,27–31] with oxygen concentrations in lung cancer tissues shown to be as low as ~1%.[29] Although GR cells analyzed in this study were established under normoxia, we hypothesized that their high basal autophagy would facilitate their survival under 1% oxygen and 1% FCS (hereafter referred to as 'hypoxic conditions'). Figure 5a shows that HCC827 GR2 and HCC4006 GR3 cells proliferated under hypoxic conditions, whereas their respective parental cells showed reduced viability in the hostile environment. To test the hypothesis mentioned above, we depleted ATG5 expression using siRNA and found that ATG5 depletion significantly reduced GR cell viability under hypoxic conditions (Figure 5b). This marked decline in viability with ATG5 depletion was probably due to impaired autophagic flux, as confirmed by a decrease in the expression of the LC3A-II form in the ATG5-depleted GR cells (Figure 5c). We also observed significantly enhanced caspase activity in ATG5-depleted GR cells compared with control cells (Figure 5d), suggesting that GR cells, at least in part, underwent apoptosis (Figures 5b and e). Beclin1 depletion caused a similar decrease in GR cell viability (data not shown) and CQ treatment dose-dependently decreased GR cell viability under hypoxic conditions (Figure 5f). Together, these results indicate that GR cells can thrive and proliferate under hypoxic conditions because of their high basal autophagy.

Autophagosomes are Formed in Untreated *EGFR*-Mutant Lung Cancer Tissues

To confirm the presence of autophagosomes in tissue samples, we collected tumor samples from 20 *EGFR*-mutant lung cancer patients, with all but one patient classified as adenocarcinoma by histology, and performed immunohistochemistry for LC3A protein using FFPE sections. We found that 14 out of the 20 *EGFR*-mutant lung carcinoma tissues were positive for LC3A by immunohistochemistry, ranging from 5 to 60% positivity (median, 10%). LC3A protein localized to the cytoplasm of carcinoma cells with a granular staining pattern, which is highly suggestive of autophago(lyso)somes (Figure 6a).[14,17,18] To confirm whether the cytoplasmic distribution of LC3A protein in carcinoma cells reflects autophagosome formation, an LC3A-positive adenocarcinoma specimen was examined with transmission electron microscopy. We found that carcinoma cells contained vesicles with a double membrane-like structure that engulfed the cytoplasm, which is characteristic of autophagosomes (Figure 6b).[14,17] LC3A-positive cells were not detected in non-tumoral tissues, except for in bronchial (or bronchiolar) epithelial cells and peripheral nerve fibers.

DISCUSSION

We have shown that two *EGFR*-mutant lung adenocarcinoma cell lines, HCC827 and HCC4006, have subpopulations of GR cells that display an EMT phenotype and can survive independent of EGFR signaling. This observation that EGFR-independent cells are inherent to *EGFR*-mutant cell lines could be one reason why EGFR TKI therapy cannot permanently eradicate *EGFR*-mutant lung cancers in the clinic. Although the GR cells analyzed here were selected from cell lines *in vitro*, studies show that some *EGFR*-mutant lung cancers with acquired TKI resistance display an EMT phenotype in the clinic.[5–8] Like *EGFR*-mutant lung cancer, chronic myeloid leukemia, which has the *Bcr-Abl* fusion gene,[32] and gastrointestinal stromal tumors, which harbors an activating mutation in the c-*kit* gene,[33] are addicted to constitutively activated tyrosine kinases. Intriguingly, these

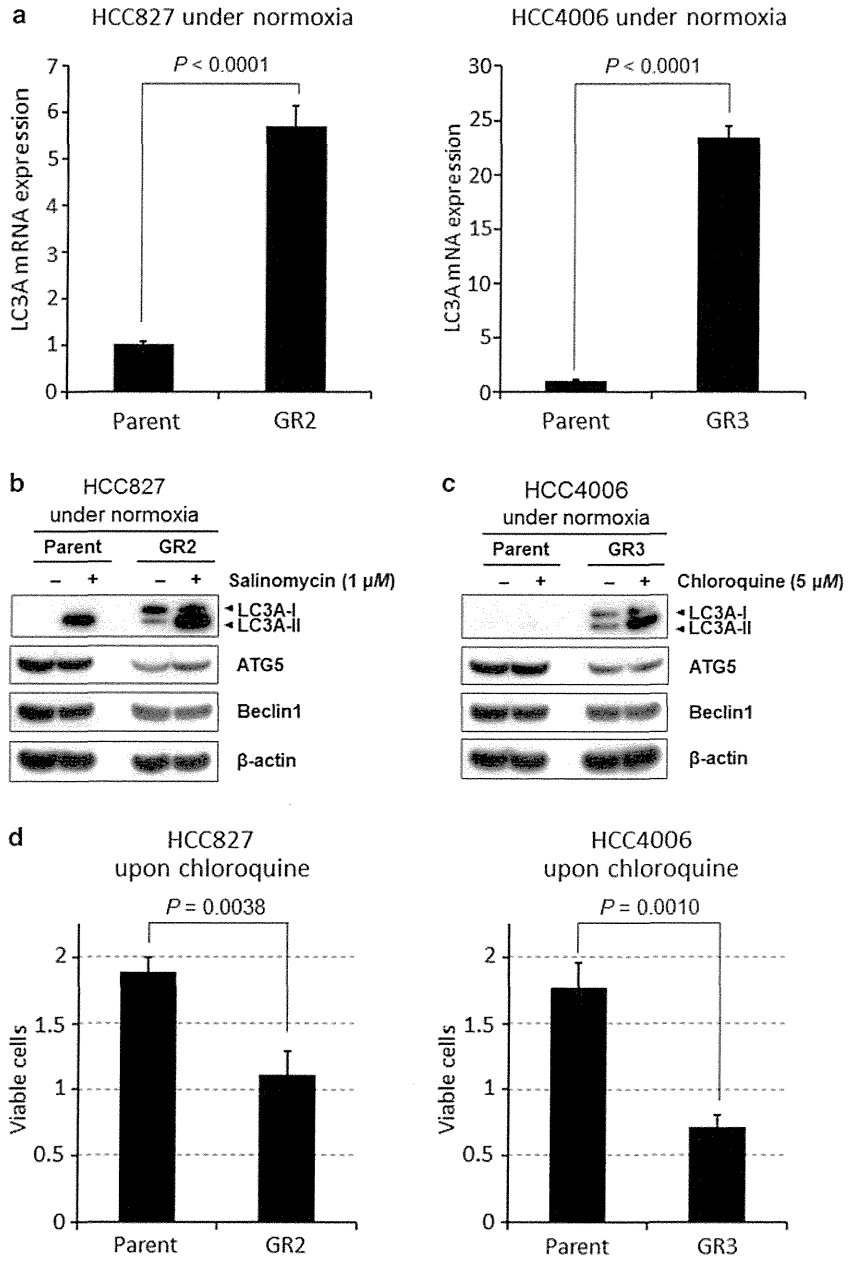

Figure 4 Gefitinib-resistant (GR) cells have higher levels of basal autophagy. (**a**) Real-time RT-PCR for the expression of LC3A mRNA in parental cells and GR cells from HCC827 or HCC4006 cells. (**b**) Western blots examining the effects of salinomycin (1 μM) for 48 h in HCC827 parental and GR2 cells. (**c**) Western blots examining the effects of chloroquine (CQ; 5 μM) for 48 h in HCC4006 parental and GR3 cells. (**d**) Viability of HCC827 or HCC4006 parental and GR cells following CQ treatment. Cells were treated with CQ (15 μM) for 72 h under normoxic conditions (20% oxygen and 10% FCS). Cell viability was assessed by trypan blue exclusion and the results were normalized to an arbitrary unit of 1.0 for viable cell number immediately before treatment. Results are expressed as the mean ($n = 3$) and s.d.

two tumors include a subset of cells that do not require the activated kinase for survival,[32,33] similar to the *EGFR*-mutant GR cells in our study.

In this study, we have also uncovered that GR cells have a higher degree of basal autophagy than their parental cells, which endows them with the potential to evade apoptosis and proliferate even under hypoxic conditions *in vitro*. These hypoxic conditions *in vitro* are reminiscent of the hostile environment within human cancer tissues.[29–31] Autophagy confers cytoprotection to cancer cells through the collection, degradation, and recycling of intracellular material in response to stress.[10–14] Here, we show that genetic and pharmacological inhibition of autophagy results in a marked decrease in GR cell viability under hypoxic conditions, and

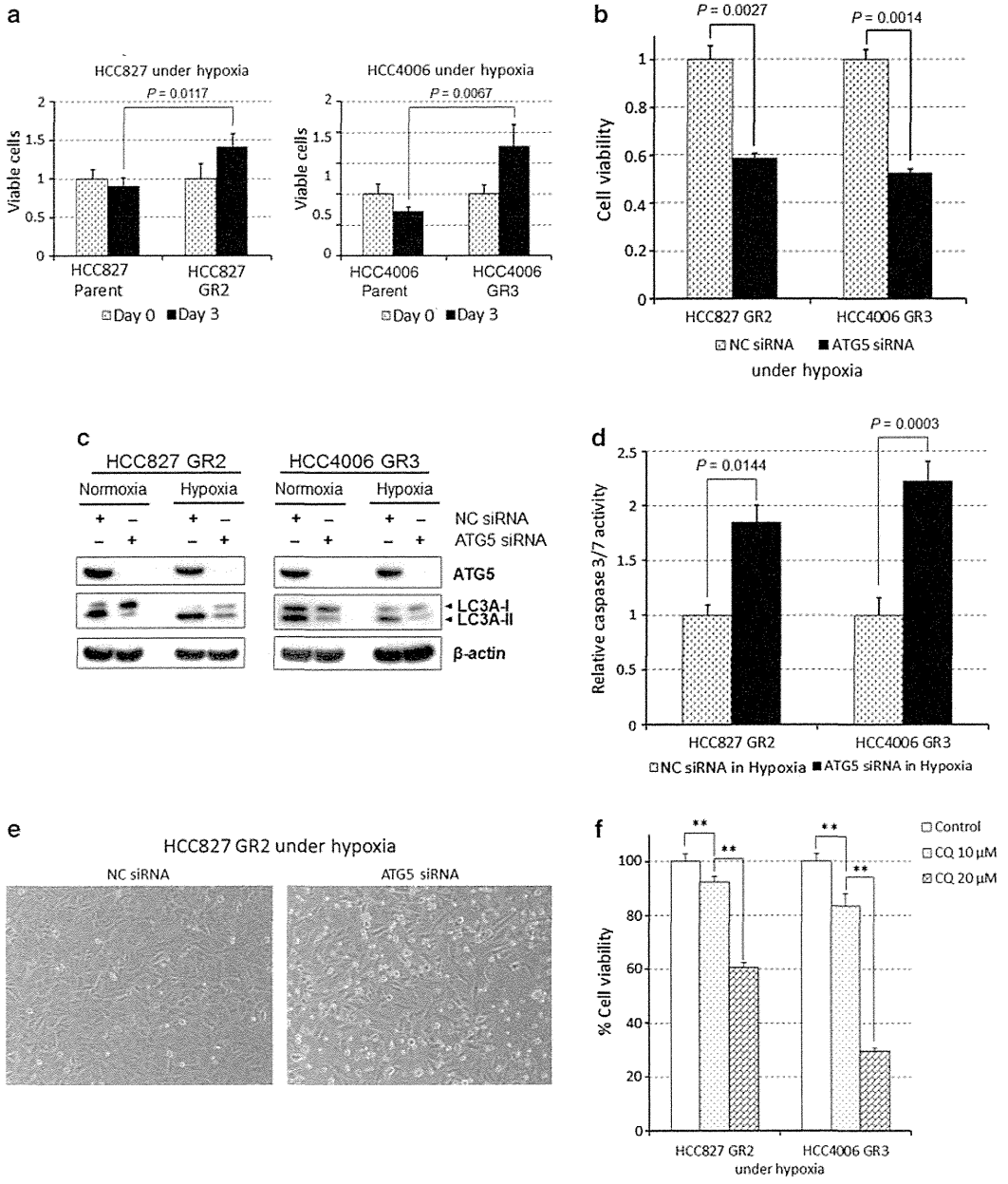

Figure 5 High basal autophagy promotes gefitinib-resistant (GR) cell survival under hypoxia. (**a**) Viability of HCC827 or HCC4006 parental and GR cells under hypoxic conditions. Cells were grown under normoxic conditions (20% oxygen and 10% FCS) for 24 h, and then cultured under hypoxic conditions (1% oxygen and 1% FCS) for another 72 h. Cell viability was assessed by trypan blue exclusion before hypoxic conditions (day 0) and 72 h after hypoxia induction (day 3). (**b**) HCC827 GR2 and HCC4006 GR3 cells were transfected with negative control (NC) small interfering RNA (siRNA; 10 nM) or ATG5 siRNA (10 nM), cultured under normoxic conditions for 24 h, and then grown under hypoxic conditions for another 72 h. Viability was determined using a WST-1 assay. (**c**) Western blots examining the effects of ATG5 depletion in HCC827 GR2 and HCC4006 GR3 cells. Cells were transfected with NC siRNA (10 nM) or ATG5 siRNA (10 nM), cultured under normoxic conditions for 24 h, and then grown under normoxic or hypoxic conditions for another 72 h. (**d**) Caspase 3/7 activity in HCC827 GR2 and HCC4006 GR3 cells under hypoxia. Cells transfected with NC siRNA or ATG5 siRNA were seeded at initial density of 0.5×10^5 cells/well and grown under normoxic conditions for 24 h, followed by hypoxic conditions for 48 h. Caspase activity was normalized to an arbitrary unit of 1.0 for the mean of three NC siRNA-transfected wells. Columns, mean ($n = 3$); bars, s.d. (**e**) Representative phase-contrast images of HCC827 GR2 cells transfected with NC siRNA or ATG5 siRNA under hypoxia, cultured as in panel **b**. (**f**) HCC827 GR2 and HCC4006 GR3 viability after chloroquine (CQ) treatment under hypoxic conditions. Cells were seeded and grown under normoxic conditions for 24 h and then untreated or treated with CQ (10 μM or 20 μM) under hypoxia for another 72 h. Viability was determined using a WST-1 assay. $^{**}P < 0.01$.

that ATG5 depletion under hypoxic conditions also causes GR cells to, at least in part, undergo apoptosis. These findings are consistent with previous reports showing that the inhibition of autophagic flux in *Ras*-mutant cancer cells results in mitochondrial dysfunction, an accumulation of cytotoxic reactive oxygen species, and increased DNA

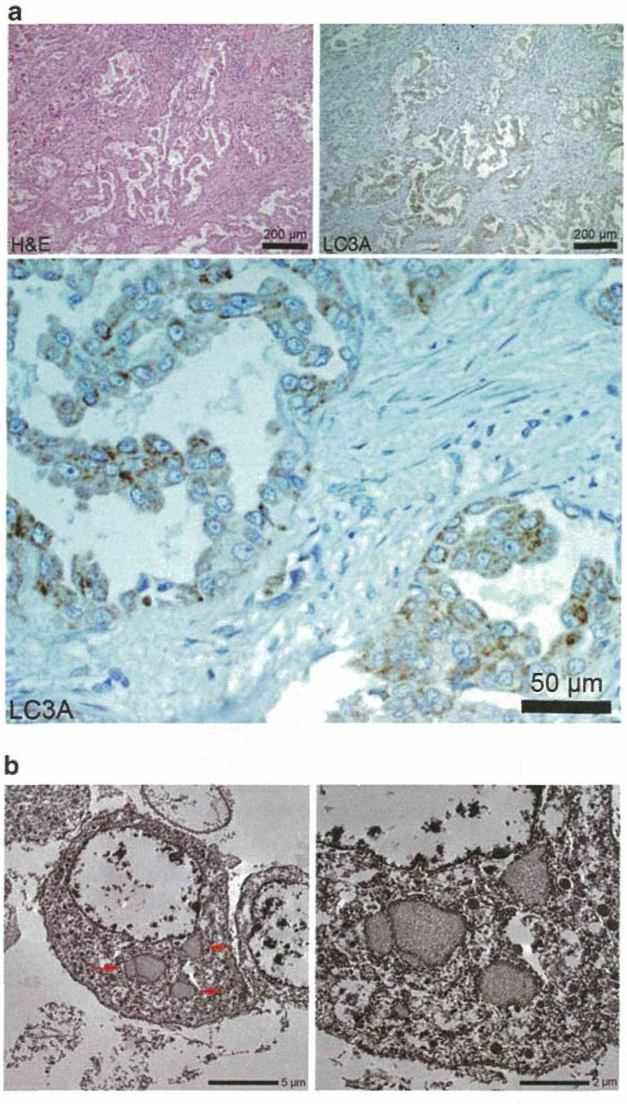

Figure 6. Autophagosomes are formed in carcinoma cells in epidermal growth factor receptor (*EGFR*)-mutant lung cancer tissues. (**a**) An untreated *EGFR*-mutant lung adenocarcinoma tissue expressing LC3A protein. (Upper left) Hematoxylin-eosin staining. (Upper right) Immunohistochemical staining for LC3A. (Lower) High-powered magnification of an LC3A-positive cancer tissue showing cytoplasmic, granular staining. (**b**) Electron microscopic analysis of the same tissue presented in panel **a**. (Left) Vesicles with a double membrane-like structure are indicated by arrows in red. (Right) High-powered magnification of the vesicles.

damage.[13,14] Autophagy has been recently reported to have a key role in the acquired resistance to erlotinib in PC9 cells, another *EGFR*-mutant lung adenocarcinoma cell line.[19] Furthermore, one report shows that erlotinib induces autophagy as well as apoptosis in parental HCC827 and HCC4006 cells, and that inhibiting autophagy significantly enhances sensitivity to erlotinib in both cell lines.[20] These findings are analogous to those already reported in chronic myeloid leukemia cells, where suppression of autophagy can potentiate apoptotic cell death induced by imatinib, a potent Abl TKI.[34] Together with our findings, these reports suggest that autophagy inhibitors could be effective not only in inducing apoptosis in EGFR TKI-resistant cells, but also in enhancing cellular susceptibility to EGFR TKIs in TKI-sensitive cells.

Most of the *EGFR*-mutant lung cancer tissues examined in our study included 5% or more carcinoma cells with cytoplasmic, granular staining of LC3A. This pattern of LC3A staining is highly suggestive of autophagosomes, and our electron microscopy results support autophagosome formation in the cytoplasm of some cancer cells.[14,17,18] However, the number of LC3A-positive carcinoma cells seems to be relatively low (median, 10%). This is probably because none of the tumor tissues examined had received neoadjuvant therapy, including EGFR TKIs, and thus the tumor tissues correspond more to the 'parental cells' in our *in vitro* experiments. All of the lung cancer tissues stained for LC3A retained an epithelial phenotype and did not involve carcinoma cells with mesenchymal-like features as seen in our GR cell culture. Hence, it remains to be elucidated to what extent autophagy is activated in *EGFR*-mutant lung cancer tissue samples that have acquired resistance to EGFR TKIs and undergone EMT.

We could not confirm previous findings that *EGFR*-mutant lung cancer cells with an EMT phenotype are dependent on AXL and EGFR for survival.[9] In HCC827 GR2 cells, AXL kinase expression was too low for detection by western blotting, and although HCC4006 GR3 cells clearly expressed AXL, they did not require the kinase for survival. In addition, while some reports show that aberrant Met activation via mutation or ligand activity secreted by stromal cells induces EMT and promotes invasion of carcinoma cells in many types of cancers,[35–37] the GR cells characterized in this study did not depend on Met signaling for survival. This is in line with previous work by others showing that EGFR TKI-resistant *EGFR*-mutant cells with an EMT phenotype were uniformly not dependent on Met kinase.[5–7] Collectively, these findings suggest that Met signaling does not have a key role in inducing or maintaining EMT of *EGFR*-mutant lung cancer cells.

In conclusion, two *EGFR*-mutant lung cancer cell lines have subsets of GR cells that have undergone EMT and can survive independent of EGFR activity. The presence of cells that are not EGFR addicted in *EGFR*-mutant lung cancer may account for the inability of EGFR TKIs to eliminate *EGFR*-mutant lung cancers. It is likely that high levels of basal autophagy in GR cells facilitate the survival of these cells under hypoxic conditions *in vitro*. Moreover, some carcinoma cells contain autophagosomes even in untreated *EGFR*-mutant lung cancer tissues *in vivo*, providing further evidence for the role of autophagy in these tissues. Considering these experimental findings and that cancer tissues usually have hypoxic regions,[29,30] targeting autophagy could be a valuable new approach to treat these cancers.

ACKNOWLEDGEMENTS

We thank Ms Kiyomi Hidano and Mr Takaaki Nikaido for their excellent electron microscopy. This work was supported in part by a Grant-in-Aid for Scientific Research (C) (24590440) from Japan Society for the Promotion of Science (to YS).

DISCLOSURE/CONFLICT OF INTEREST

The authors declare no conflict of interest.

1. Sharma SV, Bell DW, Settleman J, *et al.* Epidermal growth factor receptor mutations in lung cancer. Nat Rev Cancer 2007;7:169–181.
2. Pao W, Chmielecki J. Rational, biologically based treatment of EGFR-mutant non-small-cell lung cancer. Nat Rev Cancer 2010;10:760–774.
3. Zhou W, Ercan D, Chen L, *et al.* Novel mutant-selective EGFR kinase inhibitors against EGFR T790M. Nature 2009;462:1070–1074.
4. Nakagawa T, Takeuchi S, Yamada T, *et al.* Combined therapy with mutant-selective EGFR inhibitor and Met kinase inhibitor for overcoming erlotinib resistance in EGFR-mutant lung cancer. Mol Cancer Ther 2012;11:2149–2157.
5. Yao Z, Fenoglio S, Gao DC, *et al.* TGF-beta IL-6 axis mediates selective and adaptive mechanisms of resistance to molecular targeted therapy in lung cancer. Proc Natl Acad Sci USA 2010;107:15535–15540.
6. Suda K, Tomizawa K, Fujii M, *et al.* Epithelial to mesenchymal transition in an epidermal growth factor receptor-mutant lung cancer cell line with acquired resistance to erlotinib. J Thorac Oncol 2011;6: 1152–1161.
7. Chung JH, Rho JK, Xu X, *et al.* Clinical and molecular evidences of epithelial to mesenchymal transition in acquired resistance to EGFR-TKIs. Lung Cancer 2011;73:176–182.
8. Sequist LV, Waltman BA, Dias-Santagata D, *et al.* Genotypic and histological evolution of lung cancers acquiring resistance to EGFR inhibitors. Sci Transl Med 2011;3:75ra26.
9. Zhang Z, Lee JC, Lin L, *et al.* Activation of the AXL kinase causes resistance to EGFR-targeted therapy in lung cancer. Nat Genet 2012;44:852–860.
10. White E. Deconvoluting the context-dependent role for autophagy in cancer. Nat Rev Cancer 2012;12:401–410.
11. Kreuzaler P, Watson CJ. Killing a cancer: what are the alternatives? Nat Rev Cancer 2012;12:411–424.
12. Shen S, Kepp O, Michaud M, *et al.* Association and dissociation of autophagy, apoptosis and necrosis by systematic chemical study. Oncogene 2011;30:4544–4556.
13. Guo JY, Chen HY, Mathew R, *et al.* Activated Ras requires autophagy to maintain oxidative metabolism and tumorigenesis. Genes Dev 2011;25:460–470.
14. Yang S, Wang X, Contino G, *et al.* Pancreatic cancers require autophagy for tumor growth. Genes Dev 2011;25:717–729.
15. Zois CE, Giatromanolaki A, Sivridis E, *et al.* 'Autophagic flux' in normal mouse tissues: focus on endogenous LC3A processing. Autophagy 2011;7:1371–1378.
16. Bai H, Inoue J, Kawano T, *et al.* A transcriptional variant of the LC3A gene is involved in autophagy and frequently inactivated in human cancers. Oncogene 2012;31:4397–4408.
17. Sato K, Tsuchihara K, Fujii S, *et al.* Autophagy is activated in colorectal cancer cells and contributes to the tolerance to nutrient deprivation. Cancer Res 2007;67:9677–9684.
18. Ladoire S, Chaba K, Martins I, *et al.* Immunohistochemical detection of cytoplasmic LC3 puncta in human cancer specimens. Autophagy 2012;8:1175–1184.
19. Lee JG, Wu R. Combination erlotinib-cisplatin and Atg3-mediated autophagy in erlotinib resistant lung cancer. PLoS ONE 2012;7: e48532.
20. Li YY, Lam SK, Mak JC, *et al.* Erlotinib-induced autophagy in epidermal growth factor receptor mutated non-small cell lung cancer. Lung Cancer 2013;S0169-5002:00224–00229 (in press).
21. Verdoodt B, Vogt M, Schmitz I, *et al.* Salinomycin induces autophagy in colon and breast cancer cells with concomitant generation of reactive oxygen species. PLoS ONE 2012;7:e44132.
22. Matsukuma S, Yoshihara M, Kasai F, *et al.* Rapid and simple detection of hot spot point mutations of epidermal growth factor receptor, BRAF, and NRAS in cancers using the loop-hybrid mobility shift assay. J Mol Diagn 2006;8:504–512.
23. Matsukuma S, Saito H, Yamada K, *et al.* Simple and precise detection of UGT1A1 polymorphisms with a modified loop-hybrid mobility shift assay using Cy5-labeled loop probes. Clin Chim Acta 2011;412: 1668–1672.
24. Matsukuma S, Yoshihara M, Suda T, *et al.* Differential detection of KRAS mutations in codons 12 and 13 with a modified loop-hybrid (LH) mobility shift assay using an insert-type LH-generator. Clin Chim Acta 2011;412:1874–1878.
25. Sakuma Y, Yamazaki Y, Nakamura Y, *et al.* WZ4002, a third-generation EGFR inhibitor, can overcome anoikis resistance in EGFR-mutant lung adenocarcinomas more efficiently than Src inhibitors. Lab Invest 2012;92:371–383.
26. Sakuma Y, Yamazaki Y, Nakamura Y, *et al.* NF-κB signaling is activated and confers resistance to apoptosis in three-dimensionally cultured EGFR-mutant lung adenocarcinoma cells. Biochem Biophys Res Commun 2012;423:667–671.
27. Yang MH, Wu MZ, Chiou SH, *et al.* Direct regulation of TWIST by HIF-1alpha promotes metastasis. Nat Cell Biol 2008;10:295–305.
28. Sun S, Ning X, Zhang Y, *et al.* Hypoxia-inducible factor-1alpha induces Twist expression in tubular epithelial cells subjected to hypoxia, leading to epithelial-to-mesenchymal transition. Kidney Int 2009;75: 1278–1287.
29. Brown JM, Wilson WR. Exploiting tumour hypoxia in cancer treatment. Nat Rev Cancer 2004;4:437–447.
30. Denko NC. Hypoxia, HIF1 and glucose metabolism in the solid tumour. Nat Rev Cancer 2008;8:705–713.
31. Zhu W, Chen J, Cong X, *et al.* Hypoxia and serum deprivation-induced apoptosis in mesenchymal stem cells. Stem Cells 2006;24:416–425.
32. Corbin AS, Agarwal A, Loriaux M, *et al.* Human chronic myeloid leukemia stem cells are insensitive to imatinib despite inhibition of BCR-ABL activity. J Clin Invest 2011;121:396–409.
33. Bardsley MR, Horváth VJ, Asuzu DT, *et al.* Kit^{low} stem cells cause resistance to Kit/platelet-derived growth factor alpha inhibitors in murine gastrointestinal stromal tumors. Gastroenterology 2010;139: 942–952.
34. Bellodi C, Lidonnici MR, Hamilton A, *et al.* Targeting autophagy potentiates tyrosine kinase inhibitor-induced cell death in Philadelphia chromosome-positive cells, including primary CML stem cells. J Clin Invest 2009;119:1109–1123.
35. Boccaccio C, Comoglio PM. Invasive growth: a MET-driven genetic programme for cancer and stem cells. Nat Rev Cancer 2006;6: 637–645.
36. Gherardi E, Birchmeier W, Birchmeier C, *et al.* Targeting MET in cancer: rationale and progress. Nat Rev Cancer 2012;12:89–103.
37. Knight JF, Lesurf R, Zhao H, *et al.* Met synergizes with p53 loss to induce mammary tumors that possess features of claudin-low breast cancer. Proc Natl Acad Sci USA 2013;110:E1301–E1310.

Cancer Science
The official journal of the Japanese Cancer Association

Lung cancer with loss of BRG1/BRM, shows epithelial mesenchymal transition phenotype and distinct histologic and genetic features

Daisuke Matsubara,[1,2] Yuka Kishaba,[1] Shumpei Ishikawa,[3] Takashi Sakatani,[1] Sachiko Oguni,[1] Tomoko Tamura,[1] Hiroko Hoshino,[1] Yukihiko Sugiyama,[4] Shunsuke Endo,[5] Yoshinori Murakami,[2] Hiroyuki Aburatani,[6] Masashi Fukayama[3] and Toshiro Niki[1,7]

[1]Department of Integrative Pathology, Jichi Medical University, Shimotsuke, Tochigi; [2]Division of Molecular Pathology, Institute of Medical Science, The University of Tokyo, Minato-ku, Tokyo; [3]Department of Human Pathology, Graduate School of Medicine, The University of Tokyo, Bunkyo-ku, Tokyo; [4]Division of Pulmonary Medicine, Jichi Medical University, Tochigi; [5]Division of General Thoracic Surgery, Jichi Medical University, Shimotsuke, Tochigi; [6]Division of Genome Science, Research Center for Advanced Science and Technology, The University of Tokyo, Meguro-ku, Tokyo, Japan

(Received August 22, 2012/Revised October 30, 2012/Accepted November 6, 2012/Accepted manuscript online November 19, 2012/Article first published online January 4, 2013)

BRG1 and BRM, two core catalytic subunits in SWI/SNF chromatin remodeling complexes, have been suggested as tumor suppressors, yet their roles in carcinogenesis are unclear. Here, we present evidence that loss of BRG1 and BRM is involved in the progression of lung adenocarcinomas. Analysis of 15 lung cancer cell lines indicated that BRG1 mutations correlated with loss of BRG1 expression and that loss of BRG1 and BRM expression was frequent in E-cadherin-low and vimentin-high cell lines. Immunohistochemical analysis of 93 primary lung adenocarcinomas showed loss of BRG1 and BRM in 11 (12%) and 16 (17%) cases, respectively. Loss of expression of BRG1 and BRM was frequent in solid predominant adenocarcinomas and tumors with low thyroid transcription factor-1 (TTF-1, master regulator of lung) and low cytokeratin7 and E-cadherin (two markers for bronchial epithelial differentiation). Loss of BRG1 was correlated with the absence of lepidic growth patterns and was mutually exclusive of epidermal growth factor receptor (EGFR) mutations. In contrast, loss of BRM was found concomitant with lepidic growth patterns and EGFR mutations. Finally, we analyzed the publicly available dataset of 442 cases and found that loss of BRG1 and BRM was frequent in E-cadherin-low, TTF-1-low, and vimentin-high cases and correlated with poor prognosis. We conclude that loss of either or both BRG1 and BRM is involved in the progression of lung adenocarcinoma into solid predominant tumors with features of epithelial mesenchymal transition and loss of the bronchial epithelial phenotype. BRG1 loss was specifically involved in the progression of EGFR wild-type, but not EGFR-mutant tumors. (*Cancer Sci* 2013; 104: 266–273)

Lung cancer is the leading cause of cancer death in many developed countries, including the United States and Japan.[1,2] The identification of genetic abnormalities, such as epidermal growth factor receptor (EGFR) mutations, KRAS mutations, EML4–ALK translocation, and MET amplifications has revolutionized our understanding of the molecular mechanisms in lung cancer development.[3] However, it has become increasingly apparent that epigenetic alternations play equally important roles in tumorigenesis, and among them, chromatin remodeling factors have attracted much attention recently.[4] Indeed, identification of mutations of chromatin remodeling factors in cancer has been a major hot topic in the past 2 years.[5–8]

BRG1 and BRM, two core catalytic ATPase subunits in human SWI/SNF chromatin remodeling enzymes, have now emerged as bona fide tumor suppressor genes.[9–12] Inactivating mutations of BRG1 have been identified in 35% of non-small cell lung cancer cell lines and a subset of primary lung cancer.[9] In a mouse model of lung cancer, targeted knockout of BRG1 can affect tumor development.[10] In contrast to BRG1, mutations of BRM have rarely been identified and epigenetic silencing of BRM plays a contributory role in some cancers.[4,11] However, whether loss of BRG1 and BRM affects phenotype and differentiation of lung cancer cells remains unexplored. Furthermore, the previous studies were conducted before the discovery of EGFR mutations, and thus relationship between the EGFR status and loss of BRG1 and BRM is completely unknown.

We have recently demonstrated that lung adenocarcinoma could be classified into two groups based on the patterns of gene expression and genetic abnormalities; bronchial epithelial phenotype tumors and mesenchymal-like phenotype tumors.[13] "Bronchial epithelial phenotype" represents a group of lung adenocarcinomas with high expression of bronchial epithelial markers. This group includes thyroid transcription factor (TTF)-1 positive terminal respiratory unit (TRU) type[14] in addition to TTF-1 negative tumors with high expression of bronchial epithelial markers such as CK7 and MUC1, as detailed in our previous report.[13] Bronchial epithelial phenotype tumor exhibits high phosphorylation of EGFR and MET and frequent mutations or amplifications of EGFR, MET, and HER2. In contrast, mesenchymal-like phenotype tumors were characterized by the absence of the bronchial epithelial phenotype, triple-negative for TTF-1, MUC1, and CK7, showed no or little phosphorylation of EGFR and MET, no mutation or amplification of EGFR, MET, or HER2, and with features of epithelial mesenchymal transition (EMT), such as low E-cadherin and high FGFR1, vimentin, and ZEB1 expressions.[13] The absence of mutations or amplifications of EGFR, MET, or HER2 in mesenchymal-like phenotype tumors suggested to us that other genetic or epigenetic abnormalities may play a role in this group of tumors.

We now show in this paper that loss of expression of chromatin remodeling factors, BRG1 and BRM, correlated with features of mesenchymal-like phenotype with solid predominant histology. In particular, BRG1 loss occurred exclusively in EGFR wild-type tumors.

[7]To whom correspondence should be addressed.
E-mail: tniki@jichi.ac.jp

doi: 10.1111/cas.12065
© 2012 Japanese Cancer Association

Materials and Methods

Cell lines and medium. We used 19 non-small cell lung cancer (NSCLC) cell lines; 15 adenocarcinoma cell lines (H23, H358, H441, H522, H1395, H1648, H1650, H1703, H1795, H2087, HCC827, HCC4006, Calu3, A549, PC-3), three large cell carcinoma cell lines (H661, H1299, Lu65), and one adenosquamous cell line (H596). HCC827, H1650, H1975, PC-3, and HCC4006 were EGFR-mutated cell lines. The sources of the cell lines were described in our previous report.[13] All cell lines were maintained in RPMI1640 supplemented with 10% FCS, glutamine, and antibiotics in a humidified atmosphere with 5% CO_2 and 95% air.

Genetic and protein analysis of cell lines. The DNA, RNA, and cell lysates were prepared from cell lines by standard procedures. Experimental details of sequencing, copy number analyses, and Western blotting are given in Doc. S1. Antibodies used in western blot analysis were summarized in Table 1.

Patients and tumors. Tumor specimens were obtained from 93 patients who underwent lung cancer surgery at the Jichi medical university hospital during the period from October 2005 to June 2008. The demographic and clinicopathologic details of the patients and tumors are provided in Doc. S1.

Immunohistochemistry and evaluation. Formalin-fixed, paraffin-embedded tumor specimens were analyzed by immunohistochemistry using antibodies to BRG1, BRM, E-cadherin, cytokeratin 7, MUC1, TTF-1, p-EGF, and p-MET. The sources of antibodies, staining procedures, and methods of evaluation, are given in Doc. S1.

Mutation analyses of formalin-fixed, paraffin-embedded tissue sections. Details are shown in Doc. S1.

Bioinformatic analyses and statistics. Details are shown in Doc. S1.

Results

Characteristics of lung adenocarcinoma cell lines with loss of BRG1 and/or BRM. First, we used 15 lung cancer cell lines, for which the mutational status of BRG1 was known, to investigate the molecular features that may characterize lung adenocarcinoma cell lines with loss of BRG1. Of the 15 cell lines, six cell lines harbored BRG1 mutations and nine cell lines did not, according to previous literature,[9,11] and the Sanger COSMIC database (http://www.sanger.ac.uk/genetics/CGP/cosmic/).

Figure 1 summarizes (i) the genetic status of BRG1, EGFR, MET, HER2, BRAF, and KRAS (upper panel), (ii) gene level expressions of BRG1, BRM, TTF1, MUC1, CK7, E-cadherin, and vimentin (middle panel), and (iii) protein expression levels of BRG1, BRM, TTF1, MUC1, CK7, E-cadherin, and vimentin (lower panel) of the 15 cell lines (the microarray analysis data of 15 cell lines is located in Data S1). All six BRG1-mutated cell lines showed extreme loss of BRG1 at gene and protein levels, EMT features (low E-cadherin and high vimentin), and loss of bronchial epithelial markers (TTF-1, CK7, and MUC1). In contrast, the nine BRG1-wild type cell lines showed high expressions of BRG1, as well as high expressions of bronchial epithelial markers and E-cadherin and low expression of vimentin, at both gene and protein levels. As for gene abnormalities, BRG1-wild type cell lines showed gene abnormalities for EGFR, MET, HER2, BRAF, or KRAS, but BRG1 mutated cell lines showed no such genetic abnormalities, except for KRAS mutations.

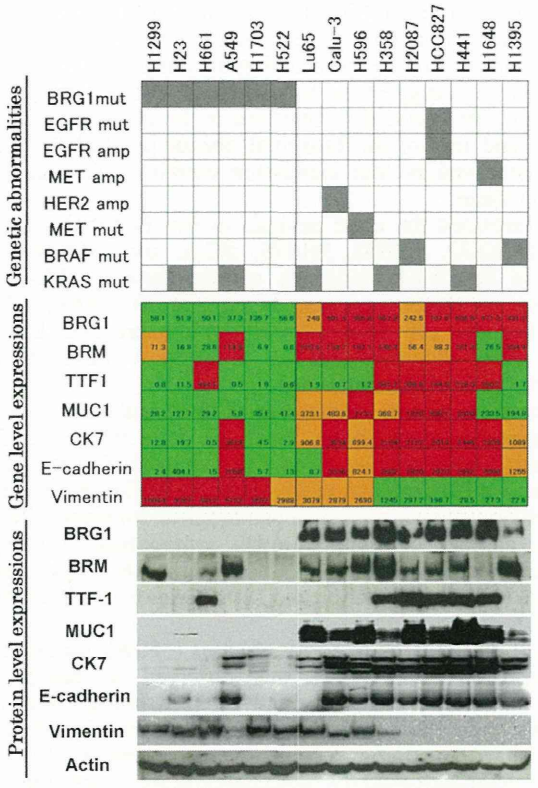

Fig. 1. Genetic status of BRG1, epidermal growth factor receptor (EGFR), MET, HER2, BRAF, and KRAS (upper panel), gene level expressions of BRG1, BRM, TTF1, MUC1, CK7, E-cadherin, and vimentin (middle panel), and protein expression levels of BRG1, BRM, TTF1, MUC1, CK7, E-cadherin, and vimentin (lower panel) of the 15 cell lines. In the upper panel, the grey box means presence of genetic abnormalities and the white box means absence of genetic abnormalities. Color indications in the middle lane are as follows: red means more than or equal to the average of each gene expression; orange: under the average and more than or equal to half the average; and green: under half the average.

We also examined the expressions of BRM in the same cell lines. Of the 15 cell lines, 10 cell lines expressed the BRM protein at modest or high levels, which was largely concordant

Table 1. Antibodies used in western blot analysis

Antibodies	Clone	Sources
BRG1 (sc-17796)	Mouse monoclonal	Santa Cruz Biotechnology (Santa Cruz, CA, USA)
BRM (A301-016A)	Rabbit polyclonal	Bethyl Laboratory (Montgomery, TX, USA)
TTF-1 (clone 8G7G3/1)	Mouse monoclonal	DAKO (Glostrup, Denmark)
Cytokeratin 7 (clone OV-TL 12/30)	Mouse monoclonal	DAKO (Glostrup, Denmark)
Vimentin (clon V9)	Mouse monoclonal	DAKO (Glostrup, Denmark)
E-cadherin (clone 36)	Mouse monoclonal	BD Biosciences (Franklin Lakes, NJ, USA)
MUC1 smaller cytoplasmic subunit	Hamster monoclonal	Lab Vision (Cheshire, UK)
Anti-rabbit IgG peroxidase conjugate		Amersham (Arlington Hights, IL, USA)
Anti-mouse IgG peroxidase conjugate		Amersham (Arlington Hights, IL, USA)
Anti-Armenian hamster IgG peroxidase conjugate		Jackson Immunoresearch (West Grove, PA, USA)

© 2012 Japanese Cancer Association